

Review article

Evolution of graphical methods for the identification of insulation faults in oil-immersed power transformers: A review

Sergio Bustamante*, Mario Manana, Alberto Arroyo, Alberto Laso, Raquel Martinez

Department of Electrical and Energy Engineering, Universidad de Cantabria, Av. Los Castros 46, Santander, 39005, Spain

ARTICLE INFO

Keywords:

Asset management
Cellulose insulation
Dissolved gas analysis
DGA interpretation
Fault identification methods
Internal incipient faults
Maintenance management
Oil insulation
Power transformer

ABSTRACT

The power transformer is one of the most important and critical assets involved in the grid and, at the same time, one of the most expensive. Several transformer condition parameters allow to assess the degradation of assets. These help in the decision-making process on the operation, repair, refurbishment, or replacement of transformers. Dissolved gas analysis (DGA) is one of the most commonly used methods to manage maintenance and establish the health index of power transformers, as well as to identify the type of fault. This paper examines and explores the studies related to graphical methods for the identification of faults in power transformers that had been developed over the last almost 50 years. The main types of faults and the sub-types presented in the analysed studies are compiled in this paper. The main differences between the methods in terms of their graphical representation, number of gases used, type of data used from the DGA results, and number of faults and sub-faults identifiable in each of them, are also presented. The application of the reviewed methods was carried out using two real DGA results.

1. Introduction

Oil-immersed power transformers are one of the most important assets in the power grid. Power transformers are used in the generation, transmission, and distribution of electricity, and they are the foundation of the power grid [1]. Power transformers are highly reliable grid assets, but like all assets, they are susceptible to failure. In addition, there are many degradation mechanisms that can occur in both components and subsystems that will reduce the useful life of the asset [2]. Some transformer condition parameters need to be assessed in order to detect asset degradation. This helps in the decision-making process regarding transformer operation, repair, refurbishment, or replacement.

Dissolved gas analysis (DGA) is one of the most commonly used methods to manage maintenance and determine the health index of power transformers [3,4]. DGA measures the concentration of gases in transformer oil. The gases normally measured are hydrogen (H_2), methane (CH_4), acetylene (C_2H_2), ethylene (C_2H_4), ethane (C_2H_6), carbon monoxide (CO), and carbon dioxide (CO_2). These gases are produced by the decomposition processes of insulation, which are caused by active faults. From the gas concentrations obtained in the DGA results, it is possible to identify the type of fault.

Traditional methods for interpreting incipient faults in power transformer oil, developed in the 1970s, used several gas ratios. These methods are the Doernenburg ratio method (DRM) [5,6], the Rogers ratio method (RRM) [7], and the IEC ratio method (IRM) [8]. The Key

Gas Method (KGM) [9], developed by Doble Laboratories (1973), uses the individual concentrations of four gases to identify the fault. It was also in this decade that the first graphical fault identification methods were developed. The first method was developed by Fallou et al. [10] and the second was the first version of the Duval triangle method (DTM 1) [11]. The first method calculates two ratios from the concentrations of 4 gases, which are plotted on a 2-axis graph to identify the type of fault. DTM 1 uses three gases corresponding to the increasing energy content or temperature of the faults to identify the type of fault in the transformer. Another graphical method, the PEM (propylene, ethylene, methane) method [12], was developed in 1979. The PEM method correlates the theoretical thermodynamic formation of C_3 hydrocarbon gases with oil temperatures in the range of 220–820 °C.

Currently, methods based on artificial intelligence (AI) or AI combined with traditional techniques are being developed to identify faults in power transformers. In [13], five different DGA techniques are used to identify the type of fault: conditional probability, clustering, DTM 1, RRM, and artificial neural network (ANN). In [14], DTM 1 and ANN are used for multi-fault diagnosis. Another DGA approach for transformer fault identification based on the combination of techniques is presented in [15], where ANN and conditional probability are used. Combinations of RRM, DRM and IRM with fuzzy logic (FL) or ANN are developed in [16] to improve diagnostic accuracy. With the same aim of improving power transformer fault diagnosis, an optimized ANN-based

* Corresponding author.

E-mail address: bustamantes@unican.es (S. Bustamante).

Nomenclature**Abbreviations**

A	Arcing
AI	Artificial intelligence
ANN	Artificial neural network
C	Possible carbonization of paper
C ₂ H ₂	Acetylene
C ₂ H ₄	Ethylene
C ₂ H ₆	Ethane
C ₃ H ₆	Propylene
C ₃ H ₈	Propane
CH ₄	Methane
CNN	Convolutional neural network
CO	Carbon monoxide
CO ₂	Carbon dioxide
D+ T	Mixture of electrical and thermal faults
D+ T1	Mixture of electrical and thermal fault T1
D+ T2	Mixture of electrical and thermal fault T2
D+ T3	Mixture of electrical and thermal fault T3
D1	Discharges of low energy
D1-H	Arcing fault (D1) in mineral oil only
D1-P	Arcing fault (D1) in paper insulation only
D2-H	Arcing fault (D2) in mineral oil only
D2-P	Arcing fault (D2) in paper insulation only
DGA	Dissolved gas analysis
DPM	Duval pentagon method
DRM	Doernenburg ratio method
DSAE	Double-stacked autoencoder method
DTM	Duval triangle method
ETRA	Electric Technology Research Association (Japan)
FGT	Universal fault gas triangle
FL	Fuzzy logic
H	Pyrolysis or thermal decomposition
H ₂	Hydrogen
D2	Discharges of high energy
HCCD	High concentration of cellulose degradation
IRM	IEC ratio method
KGM	Key gas method
LCCD	Low concentration of cellulose degradation
MCCD	Medium concentration of cellulose degradation
O	Overheating of paper or mineral oil (<250 °C)
OL	Oil leakage from OLTC
OLTC	On-load tap-changer
PD	Partial discharges
PEM	Propylene, ethylene, methane [method]
RRM	Rogers ratio method
S	Stray gassing
T1	Thermal faults (<300 °C)
T1-C	T1 with likely involvement of paper, showing carbonization
T1-O	T1 without carbonization of solid insulation
T2	Thermal faults (300–700 °C)
T2-C	T2 with high likelihood of paper involvement

T2-O	T2 but unlikely to involve solid insulation or paper carbonization
T3	Thermal faults (>700 °C)
T3-C	T3 with paper involvement (carbonization)
T3-H	T3 in mineral oil only

approach is used in [17]. A novel double-stacked autoencoder (DSAE) based diagnosis method is proposed in [18] to achieve a reliable, accurate, and faster diagnosis than other methods. Other AI techniques, such as convolutional neural network (CNN) [19] or support vector machine (SVM) [20], were also used to improve the accuracy of fault identification methods. According to [13,14,18], there is a gap in the development of fault identification methods for power transformers using AI techniques and it is still an open topic for research and development, as more reliable diagnostic methods are needed.

As indicated, the current trend is to use AI in the identification of faults in the insulation of power transformers, usually based on or supported by some of the methods already developed. Therefore, the aim of this study is to help in the selection of the fault identification method with graphical representation in which new AI-based methods will be developed. This work focuses on graphical methods of fault identification of power transformers immersed in mineral oil, the development of new and improved methods, the faults identifiable by each method, the gas concentrations used, the graphical shapes of the methods, the equations and ratios used, and future trends in fault identification. The novelty of this review lies in the comprehensive review of twenty-seven graphical fault identification methods published up to 2023 in journal articles, conference proceedings, standards/guidelines, patents and doctoral theses. This study also presents the evolution of graphical fault identification methods in terms of the number of faults they report, the number of gases they use, how DGA results are used to identify the fault, and the equations and procedures they use. This review is intended as a starting point for the development of new fault identification methods that can combine graphical methods with AI techniques.

The paper is structured as follows: Section 1 introduces the background, the contributions, and the novelty of the work. Section 2 describes the methodology followed in this work. Section 3 presents the review of all fault types identifiable using the DGA results presented in each of the methods reviewed, from the 1970s to 2023. All methods for the identification of power transformer insulation faults with graphical representation are explained in Section 4. Section 4.1 presents the procedures and equations used in each of the methods considered and shows the results of the methods when using two DGA results. Section 5 discusses the characteristics of the fault identification methods, as well as the future trend in fault identification using the DGA. Finally, Section 6 presents the conclusions.

2. Methodology

This section presents the methodology used in this study to obtain, review and extract data from the publications containing graphical methods for identifying insulation faults in oil-immersed power transformers. The flowchart of the methodology used is shown in Fig. 1.

The first step was to search for publications in scientific databases such as ScienceDirect, IEEE Xplore, and Google Scholar. The keywords used in combination to search for publications were DGA, dissolved gas analysis, power transformer, fault insulation, and graphical method. In addition to searching the scientific databases, several important standards, guidelines or manuals were consulted, including IEC and IEEE (included in the IEEE Xplore database) standards, and CIGRE technical brochures. No time limit was applied to this search, as the study aimed to collect all graphical methods of transformer fault identification.

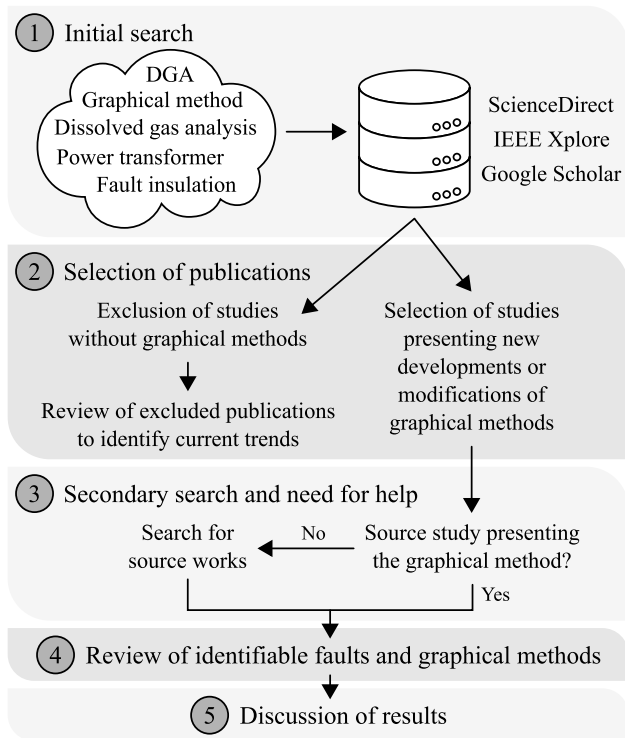


Fig. 1. Flowchart of the methodology followed in this study.

The second step was to include or exclude the articles found based on whether or not a graphical method was developed. Some of the excluded articles were related to defect identification using methods that did not present a graphical representation or developed AI-based methods. Some of the most recent publications found that develop AI-based methods are used in Section 1 to establish the current trend in this topic. As an additional task, the excluded publications were classified according to the AI techniques used for future related studies.

The initial search and classification of publications according to whether or not a new or updated graphical method was developed resulted in several methods presented in this study. However, in some cases, additional searches were necessary to find the original document in which the graphical method was first presented; this was the third step of the methodology. For example, in the case of graphical methods described in standards, it was necessary to find the original publication; in other cases, the methods presented were in publications, but the original publication describing them corresponded to patents. This step required the assistance of library technicians to locate or obtain a copy of the original publication, particularly for of old articles and conference papers.

The fourth step consisted of a review of the faults identified by each method, as well as a thorough review of each of the graphical fault identification methods and the diagnostic process used by each method.

Finally, in the fifth step, the results of the review of the graphical methods for identifying faults in the insulation of oil-immersed power transformers were discussed.

3. Power transformer faults identifiable by DGA results

At the beginning of the development of DGA in the 1970s, the first methods developed and collected in the first edition of the IEC 60599 (1978) and IEEE Std C57.104 (1978) guides, such as DRM, RRM, and IRM, identified three, eleven, and eight fault types respectively. According to the latest versions of the IEC [8] and IEEE [9] guidelines, the number of main faults in power transformer insulation has been

Table 1
Basic types of identifiable faults and gases generated [8,9].

Fault type		Gas generated				
		H ₂	CH ₄	C ₂ H ₂	C ₂ H ₄	C ₂ H ₆
Discharges of low energy	D1	•		•	◦	
Discharges of high energy	D2	•		•	◦	
Partial discharges	PD	•	◦	•		
Thermal faults (<300 °C)	T1	◦	•			•
Thermal faults (300–700 °C)	T2	◦	◦	•	•	◦
Thermal faults (>700 °C)	T3	◦		◦	•	

•: major concentration; ◦: secondary concentration; •: trace concentration.

simplified to six. These six basic types of potential faults are divided into two groups: thermal faults and electrical faults.

Thermal faults are classified according to temperature, as the effects are different. If browning of the paper is detected, it is a thermal fault in oil or paper with temperature <300 °C (T1). If there is carbonization of the paper, the temperature reached is >300 °C (T2). Finally, if there is strong evidence of carbonization of the oil, metal discoloration (800 °C) or even metal fusion (>1000 °C), it is a thermal fault >700 °C (T3).

Like thermal faults, electrical faults are identified by their effects. If X-wax is deposited on the paper, there are partial discharges (PD) of the corona type. If the effects are carbonized perforations through the paper, carbonization of the paper surface, or carbon particles in the oil, the potential fault is low energy discharges (D1) or partial discharges of the sparking type. High energy discharges (D2) in oil and/or paper are evidenced by large destruction and carbonization of paper, metal fusion at the discharge ends, large carbonization in oil, and even transformer tripping.

Table 1 shows the six basic types of fault described and the combustible gases generated in each of them.

The DTM 1 (in the third version of the method) added a new zone to the graphical representation, a mixture of thermal and electrical faults (D+ T), one of the first sub-types of faults listed in Table 2.

The creation of Duval triangles 4 (DTM 4) and 5 (DTM 5) for low temperature faults resulted in three new sub-types of thermal faults [27,28]. These three new sub-faults indicate low temperature gas generation (stray gassing – S), overheating of paper or mineral oil (O) at temperatures <250 °C, or possible carbonization of paper (C).

The fault identification method developed in [23,24], called the Gatron triangle, included a new zone indicating oil leakage or oil contamination (OL) from on-load tap-changer (OLTC) gases. This identification of oil contamination was not included in any of the earlier or later methods. Communication between the main tank and the OLTC compartment only appears in the IEC [8] and IEEE [9] guides. These guides indicate that this oil communication is possible when the C₂H₂/H₂ ratio is greater than two or three. This identification is important because gas leakage between oil compartments can influence the DGA results and the identification of transformer insulation faults [8,9,29].

The modification of DTM 1 made in [30], includes three new sub-types of D+ T faults. In this case, the type of basic thermal fault present is indicated by adding the number of the thermal fault (1, 2, or 3).

Three new zones are defined in the heptagon graph [21] to indicate cellulose (paper) degradation. These three zones indicate three levels of paper degradation, high, medium, and low degradation. When the solid insulation of power transformers is subjected to heating, the cellulose generates CO and CO₂. High concentrations of these gases are indicative of thermal ageing/degradation of the cellulose insulation [21].

A new sub-type of thermal fault was created in the first version of the Duval pentagon 2 (DPM 2) [31]. This new fault indicates thermal fault (>700 °C) in mineral oil only (T3-H). Recently, the new versions of DPM 1 and 2 [25] and DTM 1 [26], developed in 2022, allow to distinguish arcing faults in paper and in oil. These new versions split

Table 2
Sub-types of identifiable faults [8,9,21–26].

C	Possible carbonization of paper
D+ T	Mixture of electrical and thermal faults
D+ T1	Mixture of electrical and thermal fault T1
D+ T2	Mixture of electrical and thermal fault T2
D+ T3	Mixture of electrical and thermal fault T3
D1-H	Arcing fault (D1) in mineral oil only
D1-P	Arcing fault (D1) in paper insulation only
D2-H	Arcing fault (D2) in mineral oil only
D2-P	Arcing fault (D2) in paper insulation only
HCCD	High concentration of cellulose degradation
LCDD	Low concentration of cellulose degradation
MCCD	Medium concentration of cellulose degradation
O	Overheating of paper or mineral oil (<250 °C)
OL	Oil leakage from OLTC
S	Stray gassing
T1-C	Thermal fault (<300 °C) with likely involvement of paper, showing carbonization
T1-O	Thermal fault (<300 °C) without carbonization of solid insulation
T2-C	Thermal fault (300–700 °C) with high likelihood of paper involvement (probability of 80%)
T2-O	Thermal fault (300–700 °C) but unlikely to involve solid insulation or paper carbonization
T3-C	Thermal fault (>700 °C) with paper involvement in the fault (carbonization)
T3-H	Thermal fault (>700 °C) in mineral oil only

the D1 and D2 fault zones depending on whether the fault is in oil (D1-H and D2-H) or in paper (D1-P and D2-P).

Five new sub-types of faults collected in [22] combine the three basic types of thermal faults with the sub-types of low-temperature thermal faults developed in the DTM 4 and 5 [27,28], and the DPM 2 [31].

Table 2 shows the sub-types of faults discussed, which are used by the graphical fault identification methods reviewed in this paper.

4. Graphical fault identification methods

Graphical fault identification methods, based on ratios or relative percentages of gas concentrations, identify the type of fault in the transformer. In several of the methods reviewed, it is possible to see the trend of faults by plotting several DGA results over time for the same transformer. This makes these methods very interesting for utilities to use in their asset performance management systems.

One of the first graphical methods was the PEM method [12], developed in Thailand and Japan in 1979. The PEM method uses the relative percentages of propylene (C_3H_6), C_2H_4 , and CH_4 to obtain the theoretical values of the transformer oil temperature from 227 to 827 °C, as shown in Fig. 2. It should be noted that this theoretical temperature can be very different from the actual temperature, and should therefore only be used with caution [12]. It should also be noted that this method does not indicate the actual type of fault, but rather the theoretical oil temperature, so it was not included in the following parts of the review.

Twenty-six fault identification methods with graphical representation or improvements of some of them developed in the last fifty years or so were found. Fig. 3 shows the distribution by country of the main authors of the graphical fault identification methods reviewed. In the case of the method developed by Fallou et al. [10], since several authors from different countries are involved, it was decided to locate it in the country of the Working Group of the Study Committee that performed the work, in this case France.

Fig. 3 shows that the countries with the highest number of developed methods are Canada, Egypt, South Korea, and Japan. These methods include those developed by the Japan Electric Technology Association (ETRA). In addition, Fig. 4 shows the number of graphical fault identification methods developed each year during this period. From 1970 up to and including 1980, six graphical methods were developed, and the remaining twenty methods were developed from 1999 onwards.

Table 3 lists all the graphical methods analysed in this work, from oldest to newest.

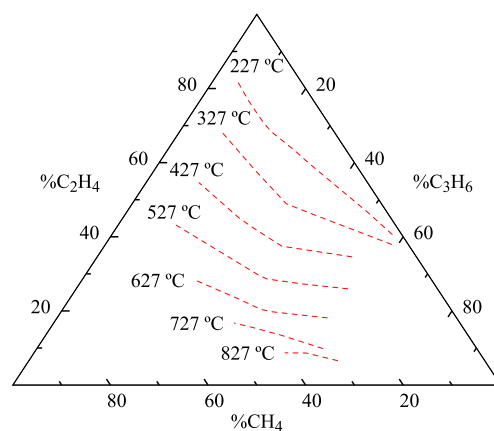


Fig. 2. PEM method [12].

One of the most important differences between the methods is the shape of the graphical representation. There are several methods that use 2-, 3-, or 8-axis charts, others that use 3-, 4-, 5-, or 7-sided polygons, one method that uses a nomogram, and another that uses a nomograph. One of the polygon methods uses a 4- or 5-sided polygon, depending on the gas concentrations converted to relative percentages. The shape of each method is shown in Table 3.

The number of gases used is also a major difference between the methods. This number varies from three to seven gases. In addition to the number of gases, Table 3 shows the individual gases used in each method analysed. The methods that use the least number of gases, in this case three gases, are those that have a triangle-shaped graphical representation and use the relative percentages of the gas concentrations. Each relative percentage of gases is plotted on each side of the triangle to identify the fault. As an exception, the Gatron triangle has a triangular shape but uses seven gas concentrations. To calculate the relative percentage it uses on one side, the Gatron triangle does the sum of five gas concentrations. There are also two other methods using seven gas concentrations: the heptagon graph [21] and the nomograph method [34,35]. The Gatron triangle uses propane (C_3H_8) and C_3H_6 as the sixth and seventh gas, while the heptagon graph and the nomograph method use CO and CO_2 ; the other five gases used being the main combustible gases measured in the DGA.

Table 3 also shows the type of data used. Several methods use the ratios of gas concentrations to plot them on 2- or 3-axis graphs, shown in the last column of Table 3 as Ratios. Most methods use relative

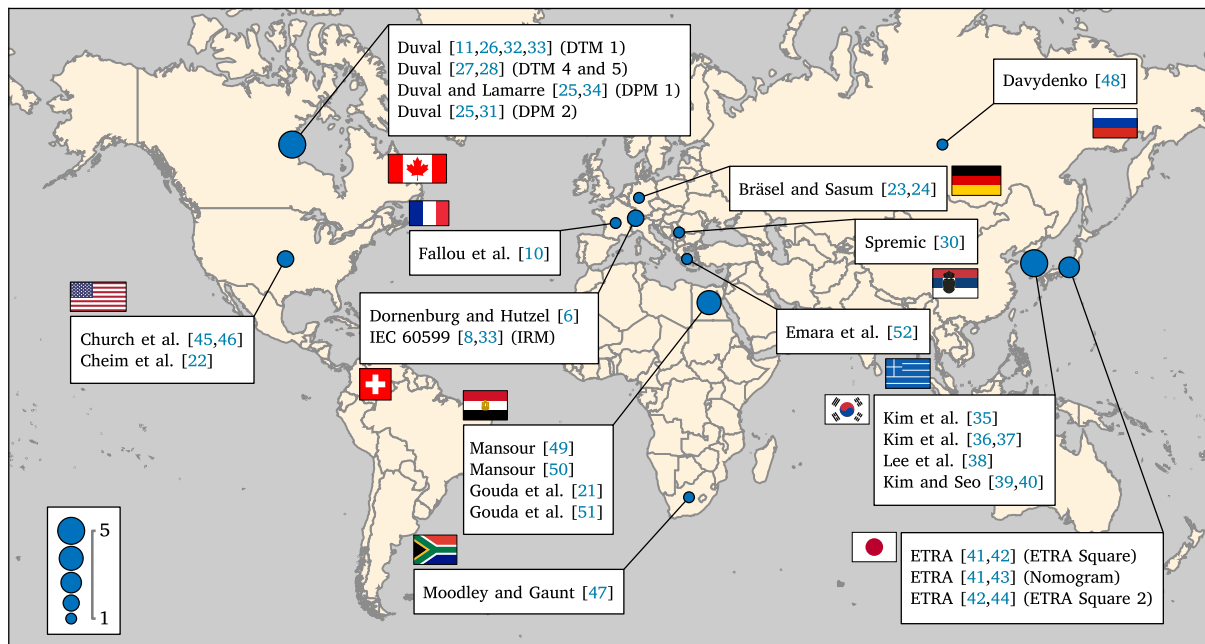


Fig. 3. Distribution by country of the main authors of the graphical fault identification methods.

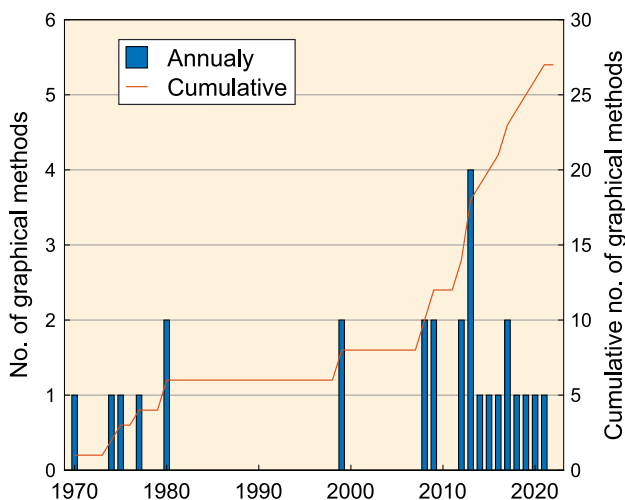


Fig. 4. Number of graphical methods developed per year and cumulative number.

percentages of gas concentrations according to the number of gases used (shown in Table 3 as Gas %). There is one method that uses three ratios of five gases, and then converts them to relative percentages, shown in Table 3 as Ratios + %. This method was developed by Gouda et al. [51] in 2019. Finally, two methods use gas concentrations in ppm without converting them into relative percentages. These two methods are the nomograph method [34] and the radar charts method [40]. The use of gas concentrations in ppm is indicated in the last column of Table 3 as ppm, but as the radar charts method additionally uses the sum of gas concentrations on one of its axes, this case is indicated in Table 3 as ppm & sum.

The main difference between all the methods is the number of faults and sub-faults they are able to identify. The number and type of faults and sub-faults that each of the graphical methods can identify is shown in Table 4. The number of faults and sub-faults identifiable by the methods ranges from three to twelve.

The method that identifies the least number of faults or sub-faults is the method presented by Fallou et al. [10], which identifies three

types. The next methods with the lowest number of identifiable faults or sub-faults are the nomograph method [34], the method developed by Doernenburg and Hutzel [6], and the DTM 4 [27,28], each of which identifies four types of fault. The method presented by Fallou et al. [10] identifies thermal decomposition, PD, and energy discharges. The nomograph method [34] identifies thermal decomposition, D2, PD, and accelerated decomposition of solid insulation. The method developed by Doernenburg and Hutzel [6] identifies D1, D2, PD, and overheating at temperatures from 200 °C to the melting point of the metal. DTM 4 [27,28] identifies few faults (PD, S, O, and C) because it is a complementary method to DTM 1. DTM 4 is used to remove uncertainty in low temperature faults in transformers.

In contrast, the methods that identify more faults or sub-faults are the ETRA nomogram [36], the combined Duval pentagons method [22], and the heptagon graph [21], which identify ten faults, and finally the radar charts method [40], which is able to identify twelve faults. In addition to identifying PD, D1, D2, T1, T2, and T3 faults, the ETRA nomogram is able to identify the following fault mixtures:

1. Sparking, creeping discharge
2. Overheating passing into PD
3. Overheating passing into arcing
4. Overheating passing into discharges

The combined Duval pentagons method, as the name suggests, is able to identify all the faults that identify DPM 1 and DPM 2, mixing the basic thermal fault types T1 and T2, and the sub-types O and C, and mixing T3 and C. In the heptagon graph, the number of faults identified increases because it is able to identify paper degradation. This method identifies three levels of degradation. In the radar charts method, the faults identified are a mixture of the faults and sub-faults. The list of faults identified by this method are:

1. Low energy PD, ageing
2. High energy PD and low temperature heating
3. PD and low temperature heating (X-wax)
4. High energy PD
5. Thermal insulation breakdown
6. Low energy PD and high temperature heating
7. Ionization insulation breakdown

Table 3
Shape, number of gases, and data type for each graphical method.

Author	Year	Shape	No.gases	Gases used	Data type
Fallou et al. [10]	1970	2-axis chart	4	H ₂ , CH ₄ , C ₂ H ₂ , C ₂ H ₄	Ratios
Duval [11,26,32,33] (DTM 1)	1974/ 1989/ 1999/ 2022	Triangle	3	CH ₄ , C ₂ H ₂ , C ₂ H ₄	Gas %
Church et al. [34,35] (Nomograph)	1975	Nomograph	7	H ₂ , CH ₄ , C ₂ H ₂ , C ₂ H ₄ , C ₂ H ₆ , CO, CO ₂	ppm
Doernenburg and Hutzler [6]	1977	2-axis chart	5	H ₂ , CH ₄ , C ₂ H ₂ , C ₂ H ₄ , C ₂ H ₆	Ratios
ETRA [36,37] (ETRA Square)	1980	2-axis chart	3	C ₂ H ₂ , C ₂ H ₄ , C ₂ H ₆	Ratios
ETRA [36,38] (Nomogram)	1980	Nomogram	5	H ₂ , CH ₄ , C ₂ H ₂ , C ₂ H ₄ , C ₂ H ₆	Ratios
IEC 60599 [8,33] (IRM)	1999	2 & 3-axis charts	5	H ₂ , CH ₄ , C ₂ H ₂ , C ₂ H ₄ , C ₂ H ₆	Ratios
ETRA [37,39] (ETRA Square 2)	1999	2-axis chart	3	C ₂ H ₂ , C ₂ H ₄ , C ₂ H ₆	Ratios
Duval [27,28] (DTM 4)	2008/ 2012	Triangle	3	H ₂ , CH ₄ , C ₂ H ₆	Gas %
Duval [27,28] (DTM 5)	2008/ 2012	Triangle	3	CH ₄ , C ₂ H ₄ , C ₂ H ₆	Gas %
Bräsel and Sasum [23,24] (Gatron triangle)	2009	Triangle	7	H ₂ , CH ₄ , C ₂ H ₂ , C ₂ H ₄ , C ₂ H ₆ , C ₃ H ₆ , C ₃ H ₈	Gas %
Davydenko [40]	2009	8-axis chart	7	H ₂ , CH ₄ , C ₂ H ₂ , C ₂ H ₄ , C ₂ H ₆ , CO, CO ₂	ppm & sum
Mansour [41]	2012	Pentagon	5	H ₂ , CH ₄ , C ₂ H ₂ , C ₂ H ₄ , C ₂ H ₆	Gas %
Moodley and Gaunt [42]	2012	Triangle	3	H ₂ , CH ₄ , CO	Gas %
Kim et al. [43]	2013	2-axis chart	5	H ₂ , CH ₄ , C ₂ H ₂ , C ₂ H ₄ , C ₂ H ₆	Ratios
Kim et al. [44,45]	2013	2-axis chart	5	H ₂ , CH ₄ , C ₂ H ₂ , C ₂ H ₄ , C ₂ H ₆	Ratios
Lee et al. [46]	2013	Square	4	H ₂ , CH ₄ , C ₂ H ₂ , C ₂ H ₄	Gas %
Lee et al. [46]	2013	2-axis chart	4	H ₂ , CH ₄ , C ₂ H ₂ , C ₂ H ₄	Gas %
Duval and Lamarre [25,47] (DPM 1)	2014/ 2022	Pentagon	5	H ₂ , CH ₄ , C ₂ H ₂ , C ₂ H ₄ , C ₂ H ₆	Gas %
Mansour [48]	2015	Pentagon	5	H ₂ , CH ₄ , C ₂ H ₂ , C ₂ H ₄ , C ₂ H ₆	Gas %
Duval [25,31] (DPM 2)	2016/ 2022	Pentagon	5	H ₂ , CH ₄ , C ₂ H ₂ , C ₂ H ₄ , C ₂ H ₆	Gas %
Spremic [30]	2017	Triangle	3	CH ₄ , C ₂ H ₂ , C ₂ H ₄	Gas %
Kim and Seo [49,50]	2017	Square	4	H ₂ , CH ₄ , C ₂ H ₄ , C ₂ H ₆	Gas %
Gouda et al. [21]	2018	Heptagon	7	H ₂ , CH ₄ , C ₂ H ₂ , C ₂ H ₄ , C ₂ H ₆ , CO, CO ₂	Gas %
Gouda et al. [51]	2019	Triangle	5	H ₂ , CH ₄ , C ₂ H ₂ , C ₂ H ₄ , C ₂ H ₆	Ratios + %
Cheim et al. [22]	2020	Pentagon	5	H ₂ , CH ₄ , C ₂ H ₂ , C ₂ H ₄ , C ₂ H ₆	Gas %
Emara et al. [52]	2021	Square and pentagon	5	H ₂ , CH ₄ , C ₂ H ₂ , C ₂ H ₄ , C ₂ H ₆	Gas %

Ratios: Ratios of gas concentrations;

Gas %: Relative percentages of gas concentrations;

ppm: Gas concentrations in ppm;

ppm & sum: Gas concentrations in ppm and sum of gas concentrations with scaling factor for CO and CO₂;

Ratios + %: Ratios of gas concentrations and then conversion to relative percentages.

8. High energy PD and high temperature heating
9. High energy discharge (arc)
10. High energy discharges and high temperature heating
11. High temperature heating, ageing of insulating materials
12. High temperature heating due to ferroresonance

Although not shown in Table 4, the only method with a graphical representation that identifies the normal state of the transformer is the one produced by Moodley and Gaunt [42,53]. The other methods do not indicate this, as it is assumed that if any gas concentration value exceeds the limits, there is a fault and the graphical method is used to identify it. In contrast, if none of the gas concentrations exceeds a threshold, the power transformer is considered to be in normal condition, and no fault identification method is required.

Fig. 5 shows the number of faults and sub-faults identifiable by the graphical methods over time. The trend (represented by the red line) shows that the number of faults and sub-faults identifiable by the methods is increasing. The black arrows shown in Fig. 5 represent the change (or not) in the number of identifiable faults in DTM 1, 4, and 5, and DPM 1 and 2 between their first and current versions. For example, the first version of DTM 1 (1974) identified four fault types, the second version (1989) six, the third version (1999) seven, while the latest version (2022) is able to diagnose nine fault types.

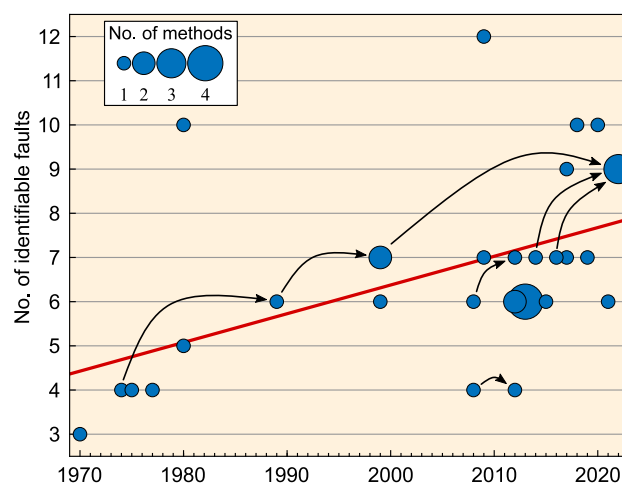


Fig. 5. Number of faults identifiable by graphical methods over time.

As discussed, there are many differences between the existing graphical fault identification methods. Table 5 shows the graphical representation of each of the methods together with a brief summary description

Table 4
Identifiable faults and sub-faults of each method.

Author	Types of faults and sub-faults																				
	PD	D1	D2	D+ T	T1	T2	T3	T1-O	T1-C	T2-O	T2-C	T3-H	T3-C	S	O	C	HCCD	MCCD	LCCD	OL	
Fallou et al. [10] ^a	✓	✓ ^j				✓ ^k															
Duval [11,26,32,33] (DTM 1) ^b	✓	✓ ^l	✓ ^m	✓ ⁿ	✓	✓ ^o	✓														
Church et al. [34,35] (Nomograph) ^c	✓		✓			✓ ^p													✓ ^q		
Doernenburg and Hutzel [6] ^a	✓	✓	✓			✓ ^r															
ETRA [36,37] (ETRA Square) ^a		✓ ^j		✓ ^s	✓	✓	✓ ^s														
ETRA [36,38] (Nomogram) ^d	✓	✓	✓ ^t	✓	✓	✓	✓														
IEC 60599 [8,33] (IRM) ^{a,e}	✓	✓	✓		✓	✓	✓														
ETRA [37,39] (ETRA Square 2) ^a	✓	✓	✓	✓ ^s	✓	✓	✓ ^s														
Duval [27,28] (DTM 4) ^b	✓													✓	✓	✓					
Duval [27,28] (DTM 5) ^b	✓					✓ ^u	✓							✓	✓	✓					
Bräsel and Sasum [23,24] (Gatron triangle) ^b	✓	✓	✓		✓	✓	✓														✓
Davydenko [40] ^f	✓		✓	✓ ^t	✓ ^t		✓ ^t														
Mansour [41] ^g	✓	✓	✓		✓	✓	✓														
Moodley and Gaunt [42] ^b	✓	✓	✓		✓	✓	✓														
Kim et al. [43] ^a	✓	✓	✓		✓	✓	✓														
Kim et al. [44,45] ^a	✓	✓	✓		✓	✓	✓														
Lee et al. [46] ^h	✓	✓	✓		✓	✓	✓														
Lee et al. [46] ^a	✓	✓	✓		✓	✓	✓														
Duval and Lamarre [25,47] (DPM 1) ^g	✓	✓ ^l	✓ ^m		✓	✓	✓							✓							
Mansour [48] ^g	✓	✓	✓		✓	✓	✓														
Duval [25,31] (DPM 2) ^g	✓	✓ ^l	✓ ^m		✓	✓	✓														
Spremic [30] ^b	✓	✓	✓	✓ ^v	✓	✓	✓					✓		✓	✓	✓					
Kim and Seo [49,50] ^h	✓	✓	✓		✓	✓	✓							✓							
Gouda et al. [21] ⁱ	✓	✓	✓	✓	✓	✓	✓										✓	✓		✓	
Gouda et al. [51] ^b	✓	✓	✓	✓	✓	✓	✓														
Cheim et al. [22] ^g	✓	✓	✓					✓	✓	✓	✓	✓	✓	✓							
Emara et al. [52] ^{g,h}	✓	✓	✓		✓	✓	✓														

^a Shapes: 2-axis.
^b Shapes: triangle.
^c Shapes: nomograph.
^d Shapes: nomogram.
^e Shapes: 3-axis.
^f Shapes: 8-axis.
^g Shapes: pentagon.
^h Shapes: square.
ⁱ Shapes: heptagon.
^j The method indicates the fault type discharge but not the energy level (D1 or D2).
^k The method indicates thermal decomposition of the oil.
^l The latest version of the method splits the D1 fault into D1-H and D1-P.
^m The latest version of the method splits the D2 fault into D2-H and D2-P.
ⁿ The first and second version of DTM 1 did not identify the fault D+ T, the current version does.
^o The first version of DTM 1 identified hot spots but did not indicate the temperature level.
^p Pyrolysis or thermal decomposition.
^q The method indicates accelerated decomposition of solid insulation.
^r The thermal fault covers temperatures from 200 °C to the melting point of the metal.
^s The method indicates that the fault can be T3 or D+ T.
^t Mixing of faults and sub-faults. Comprehensive lists of identifiable faults are provided in the text.
^u The first version of DTM 5 did not identify the fault T2, the current version does.
^v Three types of D+ T according to the three basic thermal fault types.

of the methods. The methods are listed in Table 5 from oldest to newest. The types of faults and sub-faults listed in Tables 1 and 2 are represented by the same colour in the graphical representations of each of the methods in Table 5. DTM 1, 4, and 5 are shown in Table 5 at the date of publication of the first version of the methods, but subsequently underwent changes and modifications, which are shown as the current version.

As discussed, the number of faults that the graphical methods reviewed can identify ranges from three to twelve, but it is interesting to note that the methods have increased the number of faults they

can diagnose over time. In the 1970s, the graphical methods identified three or four faults, whereas in the methods developed in the last decade this range has increased to between six and ten. This can be attributed to the splitting of different faults into subtypes, for example, depending on the location of the fault (paper or oil) or the severity of the fault (temperature-dependent thermal faults).

The most common of all the graphical methods reviewed in this study is the use of gas concentrations converted into relative percentages to the number of gases defined in each method, and the use of multiple gas ratios. Similarly, the use of combustible gases (H₂,

Table 5
Summary list of graphical methods.

Author	Year	Graph	Summary
Fallou et al. [10]	1970		This method is described in the report prepared by several members of the Working Group on Paper-oil 15.01 [10], including R. R. Rogers and E. Doernenburg (later authors of other methods for identifying faults by DGA). In this work it is shown that some of the gases generated are dissolved in the oil, so that DGA can be used to identify the type of fault. The CH_4/H_2 and C_2H_2/C_2H_4 ratios are used for this purpose. A similar graph for the interpretation of dissolved gases in the Buchholz relay is also presented in this report.
Duval [11,32] [26,33] (DTM 1)	1974/ 1989/ 1999/ 2022		The first version of the DTM 1 was developed in 1974. This version identified four types of fault. The relative percentages of three combustible gases, CH_4 , C_2H_2 , and C_2H_4 , are used to identify the fault. In 1989, Duval created the second version of the DTM 1. The identifiable faults are the six basic fault types, the zone of the first DTM 1 indicating hot spots was divided according to the temperature level of the thermal fault. The third version of DTM 1 was introduced in 1999 and identifies seven types of faults, adding a zone of mixed thermal and electrical faults to the previous six types. The temperature ranges of the three types of thermal faults were also changed. The current version of DTM 1, presented in 2022, splits the D1 and D2 fault zones according to whether the fault is in the oil (-H) or in the paper (-P). As in previous versions, the relative percentages of three combustible gases, CH_4 , C_2H_2 , and C_2H_4 , are used to identify the fault.
Church et al. [34,35]	1975		The logarithmic nomograph method was developed by J. O. Church in 1975. This method combines the concept of fault gas ratios and established threshold values. It provides a graphical representation of the fault gas data and the means to interpret its significance. The logarithmic scales and their relative positions were based on data published by Doernenburg and Strittmatter [5]. Over time, minor adjustments have been made to the placement of the logarithmic axis scales based on historical data from faulted transformers. On the logarithmic axes there are shaded and unshaded arrows. The shaded arrows correspond to the threshold criteria used by the Bureau of Reclamation, and the unshaded arrows match the threshold criteria of Doernenburg and Strittmatter [5].

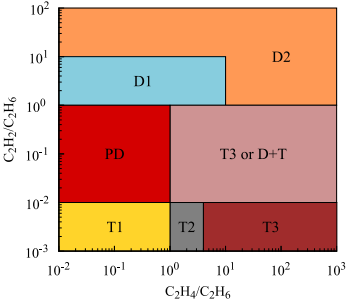
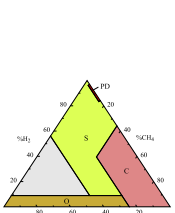
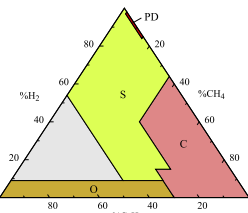
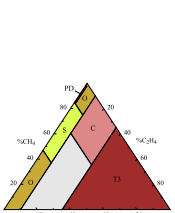
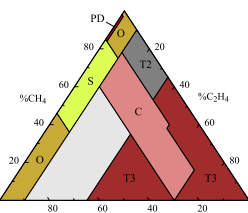
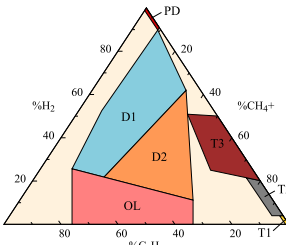
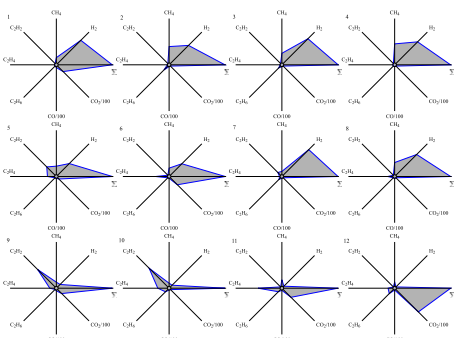
(continued on next page)

Table 5 (continued).

Author	Year	Graph	Summary
Doernenburg and Hutzl [6]	1977		In 1974, Doernenburg and Strittmatter [5] presented a first version of the DRM. Several of the DRM ratios are used in the graphical method to identify the types of faults that are important to the transformer operator. The ratios used are CH_4/H_2 , C_2H_2/C_2H_4 , and C_2H_4/C_2H_6 . As in [10], a graphical representation is also presented to identify the fault from the analysis of the free gases from the Buchholz relay.
ETRA [36,37] (ETRA square)	1980		Method developed by ETRA and collected in Japanese standards. It uses the C_2H_2/C_2H_4 and C_2H_4/C_2H_6 ratios to distinguish between electrical faults and overheating. In 1999, ETRA Square 2 [39] was introduced to complement the use of this method. The use of both methods increases the diagnostic accuracy.
ETRA [36,38] (Nomogram)	1980		This method is called nomogram or gas patterns. The fault is diagnosed by constructing the nomogram using the ratio of the gas concentrations to the gas with the highest concentration and then comparing it with the reference patterns. This method is used and included in the Russian [54,55] and Ukrainian [56] standards. In 2017, Shutenko and Jakovenko [57] developed a method that proposes the use of reference areas instead of reference images (gas patterns). Reference areas were constructed for fifty-six defects after analysing the DGA of 1,774 units with a defined defect.
IEC 60599 [8,33] (IRM)	1999		The first version of the IRM (IEC 60599:1978) was developed from the RRM [58]. The IRM uses three of the four ratios used in the RRM, the C_2H_6/CH_4 ratio was removed. The first version was based on a coding scheme of the ratios, while the second version (IEC 60599-1999) uses the ranges of the calculated ratios. This second version also includes the 2D and 3D graphical representation of the ratios.

(continued on next page)

Table 5 (continued).

Author	Year	Graph	Summary
ETRA [37,39] (ETRA square 2)	1999		<p>Second diagnostic method using a 2-axis chart developed by ETRA. Unlike the first method, the C_2H_2/C_2H_6 ratio is used on the vertical axis instead of the C_2H_2/C_2H_4 ratio. The upper part of the chart indicating discharges was separated into three zones to indicate the energy levels of the discharges (low, medium, high). As indicated, the use of both methods (ETRA square 1 and 2) increases the diagnostic accuracy.</p>
Duval [27,28] (DTM 4)	2008/ 2012	<p>1st version</p>  <p>Current version</p> 	<p>DTM 4 was developed to remove uncertainty in low temperature transformer faults, it is considered as a complement of information for DTM 1. DTM 4 should only be used when faults are first identified by DTM 1 as possible PD, T1, or T2 faults and should not be used when the faults identified by DTM 1 are D1 or D2. The new version of DTM 4 was introduced in 2012.</p>
Duval [27,28] (DTM 5)	2008/ 2012	<p>1st version</p>  <p>Current version</p> 	<p>Like DTM 4, DTM 5 was developed to remove uncertainty in low temperature transformers faults. It is an information supplement to DTM 1. DTM 5 should only be applied to faults identified by DTM 1 as T2 or T3. It should not be applied to faults identified by DTM 1 as D1 or D2. The new version of DTM 5 was introduced alongside DTM 4 in 2012.</p>
Bräsel and Sasum [23,24] (Gatron triangle)	2009		<p>Bräsel and Sasum developed a graphical method called the universal fault gas triangle (FGT) or Gatron triangle. The use of the graphical method to define the fault is similar to DTM 1, 4 and 5, but the FGT uses seven hydrocarbon gas concentrations instead of three. The gases are placed on the sides of the triangle to indicate the main fault types. H_2 for partial discharges, C_2H_2 for electrical discharges, and the remaining 5 hydrocarbon gases for thermal faults.</p>
Davydenko [40]	2009		<p>The method developed by Davydenko is used to determine the condition of oil-filled high-voltage equipment. In this graphical method, the concentrations of seven gases are plotted on an 8-axis chart, with the eighth axis plotting the sum of the seven gases according to the equation shown later in the paper. By plotting the concentrations and the sum of gases on the chart, a pattern is obtained. This pattern should be compared with the twelve reference patterns developed by Davydenko to identify the type of fault.</p>

(continued on next page)

Table 5 (continued).

Author	Year	Graph	Summary
Mansour [41]	2012		In 2012, Mansour presented the first pentagon-shaped fault identification method. This method uses the five combustible gases obtained in the DGA. Through this method it is possible to identify the six main types of faults. The relative percentages of the five combustible gases are calculated. It is assumed that these relative percentages are located at each of the heads of the pentagon, so it is necessary to calculate the centre of mass of these percentage concentrations to identify the type of fault.
Moodley and Gaunt [42]	2012		The work performed by Moodley states that incipient faults in power transformers usually start as low-energy faults [42,53]. Therefore, Moodley and Gaunt developed this method to identify when a power transformer is going from a normal to an abnormal state. This method uses the concentrations of H ₂ , CH ₄ , and CO. In this work it is stated that under normal conditions the relative percentages of H ₂ and CH ₄ are 20%, and 80% is CO.
Kim et al. [43]	2013		The authors of the paper presenting the graphical method belong to Hyosung Corporation, except for one of them, Michel Duval. This method is covered by two patents, granted in 2013 [44] and 2017 [45]. In this work, ten gas ratios were used to analyse the patterns of the results and to determine whether they could be used to discriminate between faults. The ratios used were CH ₄ /H ₂ , C ₂ H ₂ /C ₂ H ₄ , C ₂ H ₂ /CH ₄ , C ₂ H ₆ /C ₂ H ₂ , C ₂ H ₄ /C ₂ H ₆ , C ₂ H ₄ /CH ₄ , C ₂ H ₆ /CH ₄ , C ₂ H ₄ /H ₂ , C ₂ H ₆ /H ₂ , and C ₂ H ₂ /H ₂ . The first five ratios are those used in the DRM, IRM, and RRM. The last five ratios were not used in any method or standard at the time. They then combined fifteen gas-ratio combinations using the first six gas ratios to define the best combinations for fault identification. They decided to use three gas ratio combinations (R1–R2, R2–R5, and R5–R6) and constructed the charts on the left from 122 DGA results with identified faults. The graphical method consists of four 2-axis charts.
Kim et al. [44,45]	2013		This graphical method is covered by two Hyosung Corporation patents [44,45]. In this method, four gas ratios are used and combined into two combinations of gas ratios to create two graphs. Using these two graphs, it is possible to identify the fault of the six main types of failure.
Lee et al. [46]	2013		In addition to the work presented in [46], this graphical method is covered by five patents [49,50,59–61] of Hyosung Corporation. This method uses the relative percentage of H ₂ , CH ₄ , C ₂ H ₂ , and C ₂ H ₄ to identify the fault according to the six main types of faults in a transformer. It uses H ₂ as the gas corresponding to low energy electrical faults, CH ₄ for low energy thermal faults, C ₂ H ₄ for high energy thermal faults, and C ₂ H ₂ for high energy electrical faults.

(continued on next page)

Table 5 (continued).

Author	Year	Graph	Summary
Lee et al. [46]	2013		<p>The graphical method presented in [46] is also covered by three Hyosung Corporation patents [60–62]. This method uses four combinations of the relative percentages of two gases on 2-axis plots. According to the authors, the combination of the relative percentages of H₂ and CH₄ corresponds to low energy electrical faults and low temperature thermal faults. The combination of the relative percentages of H₂ and C₂H₂ corresponds to low and high energy electrical faults. The combination of the relative percentages of C₂H₂ and C₂H₄ corresponds to high energy electrical faults and high temperature thermal faults. And the combination of the relative percentages of CH₄ and C₂H₄ corresponds to low and high temperature thermal faults. As a result, the fault diagnosed for each combination may be different. To overcome this, the authors present the weight values of the faults diagnosed for each combination to perform the fault diagnosis.</p>
Duval and Lamarre [25,47] (DPM 1)	2014/2022	<p>First version</p> <p>Current version</p>	<p>The method uses the relative percentages of the five main hydrocarbon gases analysed by DGA in a pentagonal representation. The carbon oxides CO and CO₂ are not used in this method and must be evaluated separately as in other methods. Each relative percentage of each gas is plotted on its corresponding axis, giving five different points. The centroid of the irregular polygon plotted from these five points is then mathematically calculated. The location of this centroid represents the result of the DGA diagnosis in DPM 1. The difference between the two versions is that the current version splits the D1 and D2 fault zones in two to indicate whether the fault is in the oil (-H) or in the paper (-P).</p>
Mansour [48]	2015		<p>As in Mansour's first pentagon [41], the five hydrocarbon gases obtained in the DGA are used. This method makes it possible to identify the six main types of failure. The procedure is similar to the first pentagon in that the relative percentages of the five combustible gases are calculated, assumed to be at each head of the pentagon, so that the centre of mass of these percentage concentrations must be calculated to identify the type of fault. The difference with Mansour's first pentagon is the arrangement of the zones indicating the type of fault.</p>

(continued on next page)

Table 5 (continued).

Author	Year	Graph	Summary
Duval [25,31] (DPM 2)	2016/2022	<p>First version</p> <p>Current version</p>	<p>DPM 2 was developed in a similar way to DTM 4 and 5 [27,28] to remove the uncertainty in low temperature transformer faults. The three sub-types of faults (S, O, and C) that can be identified in DTM 4 and 5 can also be identified in DPM 2. In addition, there is a new zone (T3-H) that indicates T3/T2 faults in oil only. When plotting the evolution of DGA points over time in DPM 1, if any of them are in thermal zones, the method is switched to DPM 2. Like the current versions of DPM 1 and DTM 1, the current version of DPM 2 splits the D1 and D2 fault zones to indicate whether the fault is in the oil (-H) or in the paper (-P).</p>
Spremic [30]	2017		<p>The work developed by Spremic aims to improve the DTM 1. The author states that a large number of failure cases supported by DGA results, visual inspection, and laboratory experiments, yielded knowledge that a significant number of DGA cases are D+T failures. According to the DGA database used by the author, a small percentage of the DGA results with confirmed D+T failures fall into the DTM 1 D+T zone. On the left side of the triangle, the author uses the relative percentage of the sum of CH₄ and C₂H₆, unlike DTM 1. The second difference concerns the layout of the zones indicating the type of fault. Pure fault types D1 and D2 are grouped in small zones. Mixed thermal and discharge faults are frequent, so they represent large areas within the triangle, divided by the temperature level of the thermal fault. Pure thermal faults are located at or very close to the right edge of the triangle.</p>
Kim and Seo [49,50]	2017		<p>This graphical method is covered by two Hyosung Corporation patents [49,50]. The method uses the relative percentage of H₂, CH₄, C₂H₄ and C₂H₆ to identify four major fault types (three types of thermal faults and partial discharges), a zone indicating high and low energy discharges (D1/D2), and stray gassing. It uses H₂ as the gas corresponding to low energy electrical faults, C₂H₄ for high energy thermal faults, C₂H₆ for high energy electrical faults, and CH₄ for low energy thermal faults. According to the flowchart in the patents [49,50], this method is combined with the graphical method of the same shape presented in [46] if the result obtained is not stray gassing.</p>
Gouda et al. [21]	2018		<p>Gouda et al. present a new graphical method using the shape of a heptagon based on the seven gases produced in the decomposition of transformer oil due to faults. The authors used 452 DGA results to create the zones for the different fault types. This work takes into account the concentrations of H₂ and C₂H₆, and the ageing and failure of solid insulation indicated by the concentrations of CO and CO₂, which are not usually used.</p>

(continued on next page)

Table 5 (continued).

Author	Year	Graph	Summary
Gouda et al. [51]	2019		The authors point out that the most commonly used fault identification method is DTM 1, but unfortunately the effects of C ₂ H ₆ and H ₂ are not included in DTM 1, despite their importance in diagnosing certain types of faults. This work presents a new graphical triangle method using new gas concentration ratios. These ratios are obtained by considering the five combustible gases. The ratios are then converted into relative percentages to be plotted on the triangle. Like the DTM, this method identifies the six main fault types plus DT. The authors used 383 DGA results to create the zones for the different fault types.
Cheim et al. [22]	2020		This method combines DPM 1 and 2. It aims to facilitate automatic fault identification by software and to exploit the full capability of the two original pentagons. The combination of the pentagons results in a reduced number of fault zones, ten as opposed to fourteen for the original pentagons (although zones PD, S, D1 and D2 are common to DPM 1 and 2). This reduction in zones eliminates the need to resolve two separate pentagons when identifying thermal faults (this is when DPM 2 is used [31]). In this combined pentagon method, the thermal faults T1 and T2 are doubled according to overheating (-O) or carbonization (-S) of paper. Thermal fault T3 is also doubled according to whether the fault is only in the oil (-H) or there is carbonization of the paper (-C).
Emara et al. [52]	2021		Emara et al. present a new fault identification method based on five combustible gases (H ₂ , CH ₄ , C ₂ H ₂ , C ₂ H ₄ , and C ₂ H ₆) and using two different shapes. The relative percentage of C ₂ H ₂ determines which shape to use. According to the authors, since the temperature for small amounts of C ₂ H ₂ to be generated is between 500 and 700 ° C, in the case of T1 faults, the C ₂ H ₂ concentrations are small enough and therefore negligible for fault identification. Four gases (H ₂ , CH ₄ , C ₂ H ₄ , and C ₂ H ₆) and the square shape are therefore used to identify T1 faults, in addition to PD and part of the thermal faults (T2 and T3). In contrast, C ₂ H ₂ is mainly produced in the D1 and D2 faults, so the pentagon shape is used for this case. This pentagon shape is also used to identify the remaining faults of PD, T2 and T3. To test the accuracy of the two-shape graphical method, the authors used 375 DGA results and obtained an accuracy of 78.93%.

CH₄, C₂H₂, C₂H₄, and C₂H₆) for fault diagnosis is the most common, with only four of the twenty-seven methods reviewed using CO or CO₂. Thus, the use of combustible gases remains the dominant preference for fault identification.

4.1. Procedures and equations of the graphical fault identification methods

This section presents the procedures and equations used by the graphical fault identification methods described in the previous section. Fig. 6 summarizes the flowchart to be followed in each of the graphical methods. The first step is to check whether any of the gas concentrations exceed the set threshold. The relative percentages or gas ratios are then calculated if the method uses them. The next step is to create the graphical representation. Finally, the type of fault in the transformer is determined directly from the graphical representation or by comparison with reference patterns.

Since the method developed by Moodley and Gaunt [42] also indicates the normal condition of the transformer, even if the answer to the first question in the flowchart in Fig. 6 is No, it is necessary to continue as if the answer were Yes in order to obtain the result provided by the method.

Table 6

DGA results used in the application of graphical fault identification methods (ppm).

DGA no.	H ₂	CH ₄	C ₂ H ₂	C ₂ H ₄	C ₂ H ₆	CO	CO ₂
1	31	155	1	45	321	728	2,645
2	157	20	144	113	5	490	6,253

The DGA results of two oil samples from two in-service power transformers (Table 6) were used in each of the graphical methods to better illustrate the procedure, application of the equations, and interpretation of the results of each method.

The application of the nomograph method to the two DGA samples is shown in Fig. 7. On each of the logarithmic vertical axes, the value of the measured concentration of each of the gases, given at the bottom of the axis, must be placed.

The values of C₂H₆ and CH₄ concentrations of sample DGA 1 exceed the two thresholds established in the nomograph (indicated by shaded and unshaded arrows), so it is correct to apply the method. Similarly, for sample DGA 2, the gas concentration exceeding both thresholds is C₂H₂, and C₂H₄ exceeds one of the two thresholds, so it is also correct to use the nomograph.

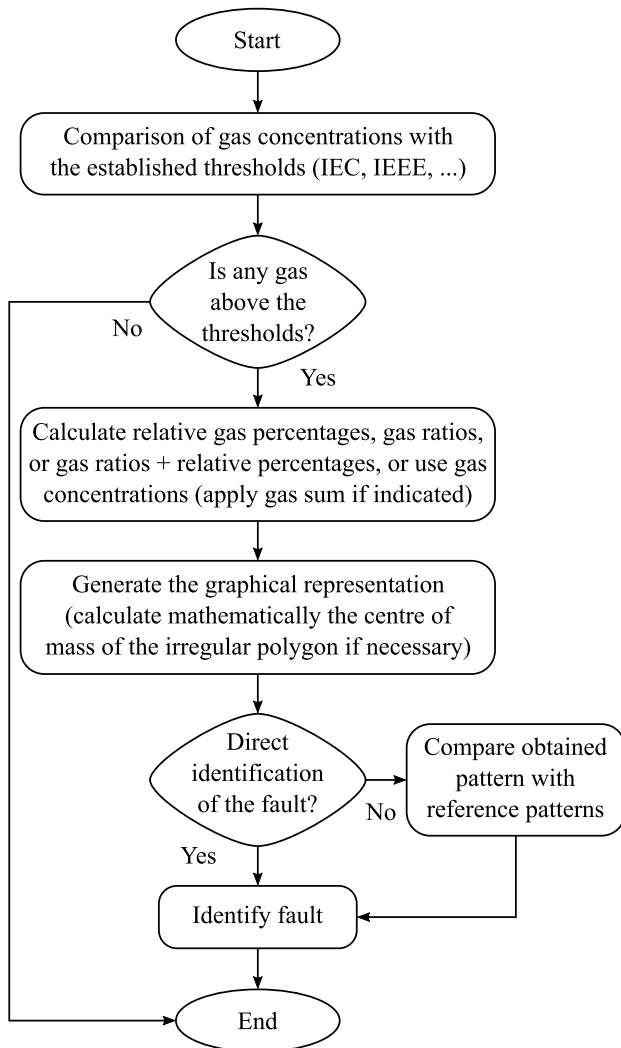


Fig. 6. Summary flowchart of fault identification methods.

The successive points marked on the axes are then joined. By observing the slopes obtained by joining the points and comparing them with those at the bottom of the nomograph, it is possible to identify the type of fault. A negative slope of the line joining the CO and CO₂ concentrations indicates an accelerated decomposition rate of the solid insulation due to the high temperatures associated with a fault.

DGA sample number 1, represented by the red dashed line in Fig. 7, was identified in the nomograph as H, pyrolysis or thermal decomposition. In addition, a negative slope of the line connecting the CO and CO₂ concentrations indicates an accelerated decomposition rate of the solid insulation. DGA sample number 2, represented by the blue dashed line in Fig. 7, was identified in the nomograph as A, arcing.

The procedures and equations of the remaining methods were grouped according to the shape of the graphical methods studied in this review. Table 7 lists the procedures and equations of the seven triangular-shaped graphical methods.

In four of the seven methods, the relative percentage of three gases is calculated and each relative percentage of gas is placed on each side of the triangle. These methods are DTM 1 [11,32,33], 4, and 5 [27,28], and the method developed by Moodley and Gaunt [42].

Something similar happens in the method developed by Bräsel and Sasum [23,24] and in the method developed by Spremic [30]. These two methods use the sum of several gas concentrations to calculate the relative percentage used on one side. In Bräsel and Sasum [23,24] the

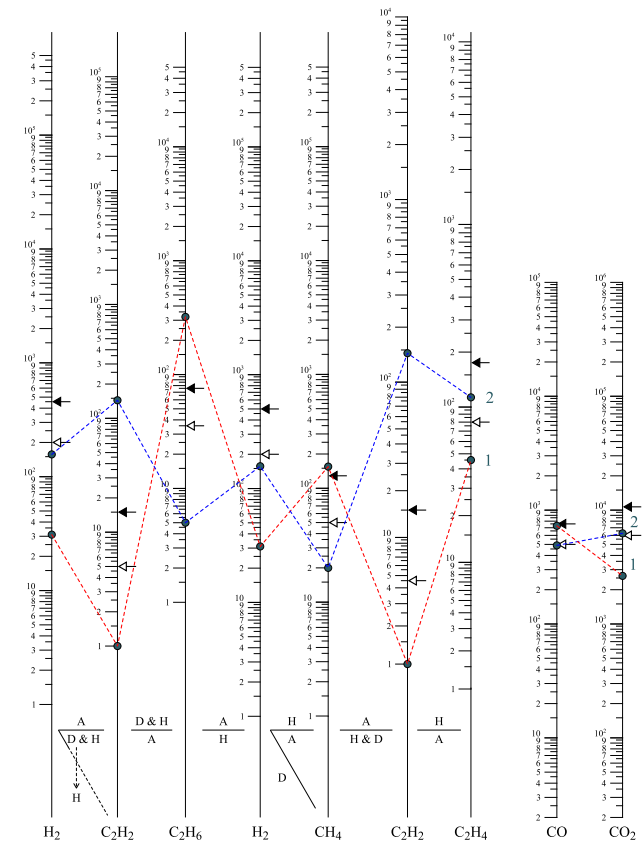


Fig. 7. Example of the application of the nomograph method.

concentrations of CH₄, C₂H₂, C₂H₆, C₃H₆, and C₃H₈ are added together, and in Spremic [30] the concentrations of CH₄ and C₂H₆ are added together.

The third way of using the gas concentrations in the triangular-shaped methods is the method developed by Gouda et al. [51]. In this method, three ratios are calculated where the main gases are CH₄, C₂H₂, and C₂H₄; and then the relative percentages of these three ratios are calculated and placed on each side of the triangle.

Table 8 shows the pentagon-shaped methods. In these five methods, there are two ways to identify the type of fault.

The first is the one used by Mansour's pentagons [41,48]. In this case, the calculated relative percentages of five gases are placed on the heads of the pentagon. Using the relative coordinates of each of the heads of the pentagon and the relative percentages in the equations in Table 8, it is possible to obtain the relative coordinates that identify the type of fault.

The other way use the procedure described by Duval and Lamarre [47]. On the axes connecting the centre of the pentagon to the heads of the pentagon (the heads of the pentagon represent the relative percentage equal to 40% for each of the gases), the relative percentages of the five gases are placed to obtain an irregular pentagon. The centroid of this irregular pentagon is the point that indicates the type of fault in the power transformer.

The procedures and equations for methods using 2-, 3-, or 8-axis charts, or a nomogram are given in Table 9. With this type of graphical method there are two ways of identifying the fault.

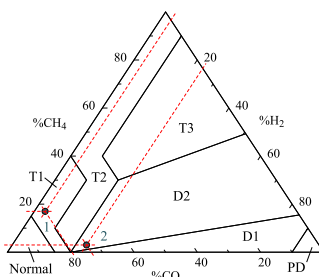
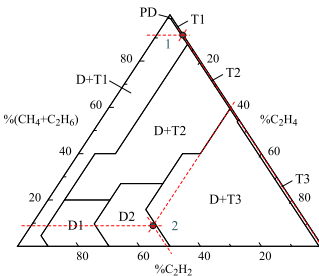
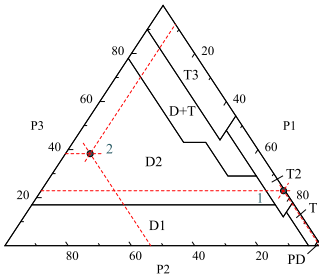
The first way is to plot the gas ratios on 2- or 3-axis graphs. In some of the methods using this first way, the fault present is obtained by using one or two charts with different gas ratios at the same time. However, there are others, such Kim et al. [43] and Lee et al. [46], which follow a flowchart based on the result of the first graph in order to identify the type of fault.

Table 7
Procedures and equations for triangular-shaped graphical methods.

Author	Year	Graph	Equation
Duval [11,32] [26,33] (DTM 1)	1974/ 1989/ 1999/ 2022	<p>1st version</p>	$\%C_2H_2 = \frac{100 \cdot x}{x+y+z}$ $\%C_2H_4 = \frac{100 \cdot y}{x+y+z}$ $\%CH_4 = \frac{100 \cdot z}{x+y+z}$ <p>x, y, and z are the concentrations of C_2H_2, C_2H_4, and CH_4 (ppm) respectively (No. 1: $\%C_2H_2 = 0.5\%$, $\%C_2H_4 = 22.4\%$, $\%CH_4 = 77.1\%$; No. 2: $\%C_2H_2 = 52\%$, $\%C_2H_4 = 40.8\%$, $\%CH_4 = 7.2\%$)</p>
		<p>2nd version</p>	
		<p>3rd version</p>	
		<p>Current version</p>	
Duval [27,28] (DTM 4)	2008/ 2012	<p>1st version</p>	$\%C_2H_6 = \frac{100 \cdot x}{x+y+z}$ $\%CH_4 = \frac{100 \cdot y}{x+y+z}$ $\%H_2 = \frac{100 \cdot z}{x+y+z}$ <p>x, y, and z are the concentrations of C_2H_6, CH_4, and H_2 (ppm) respectively (No. 1: $\%C_2H_6 = 63.3\%$, $\%CH_4 = 30.6\%$, $\%H_2 = 6.1\%$; No. 2: Not identified – Method not used for the type of faults identified in DTM 1 as D1 or D2)</p>
		<p>Current version</p>	
Duval [27,28] (DTM 5)	2008/ 2012	<p>1st version</p>	$\%C_2H_6 = \frac{100 \cdot x}{x+y+z}$ $\%C_2H_4 = \frac{100 \cdot y}{x+y+z}$ $\%CH_4 = \frac{100 \cdot z}{x+y+z}$ <p>x, y, and z are the concentrations of C_2H_6, C_2H_4, and CH_4 (ppm) respectively (No. 1: $\%C_2H_6 = 61.6\%$, $\%C_2H_4 = 8.6\%$, $\%CH_4 = 29.8\%$; No. 2: Not identified – Method not used for the type of faults identified in DTM 1 as D1 or D2)</p>
		<p>Current version</p>	
Bräsel and Sasum [23,24]	2009		$\%H_2 = \frac{100 \cdot x}{x+y+z}$ $\%C_2H_4 = \frac{100 \cdot y}{x+y+z}$ $\%CH_4+ = \frac{100 \cdot z}{x+y+z}$ <p>x and y are the concentrations of H_2 and C_2H_4 (ppm) respectively, and z is the sum of concentrations of CH_4, C_2H_2, C_2H_6, C_3H_6, and C_3H_8 (ppm) (The concentrations of C_3H_6 and C_3H_8 were not available in the DGA results used, so it was not possible to perform the graphical representation of the method or to identify the type of fault)</p>

(continued on next page)

Table 7 (continued).

Author	Year	Graph	Equation
Moodley and Gaunt [42]	2012		$\%H_2 = \frac{100 \cdot x}{x+y+z}$ $\%CH_4 = \frac{100 \cdot y}{x+y+z}$ $\%CO = \frac{100 \cdot z}{x+y+z}$ <p>x, y, and z are the concentrations of H_2, CH_4, and CO (ppm) respectively (No. 1: $\%H_2 = 3.4\%$, $\%CH_4 = 17\%$, $\%CO = 79.6\%$; No. 2: $\%H_2 = 23.5\%$, $\%CH_4 = 3\%$, $\%CO = 73.5\%$)</p>
Spremic [30]	2017		$\%C_2H_2 = \frac{100 \cdot x}{x+y+z}$ $\%C_2H_4 = \frac{100 \cdot y}{x+y+z}$ $\%(CH_4 + C_2H_6) = \frac{100 \cdot z}{x+y+z}$ <p>x and y are the concentrations of C_2H_2 and C_2H_4 respectively, and z is the sum of concentrations of CH_4 and C_2H_6 (ppm) (No. 1: $\%C_2H_2 = 0.2\%$, $\%C_2H_4 = 8.6\%$, $\%(CH_4 + C_2H_6) = 91.2\%$; No. 2: $\%C_2H_2 = 51.06\%$, $\%C_2H_4 = 40.07\%$, $\%(CH_4 + C_2H_6) = 8.87\%$)</p>
Gouda et al. [51]	2019		$R1 = \frac{CH_4}{CH_4 + C_2H_6 + C_2H_2 + C_2H_4}$ $R2 = \frac{C_2H_2}{H_2 + CH_4 + C_2H_6 + C_2H_4}$ $R3 = \frac{C_2H_4}{H_2 + CH_4 + C_2H_6 + C_2H_2}$ $P1 = \frac{R1 \cdot x \cdot 100}{S}$ $P2 = \frac{R2 \cdot x \cdot 100}{S}$ $P3 = \frac{R3 \cdot x \cdot 100}{S}$ $S = R1 + R2 + R3$ <p>H_2, CH_4, C_2H_2, C_2H_4, and C_2H_6 are gas concentrations (ppm) (No. 1: $R1 = 0.4\%$, $R2 = 19.4\%$, $R3 = 66.8\%$, $P1 = 13.4\%$, $P2 = 13.4\%$, $P3 = 13.4\%$; No. 2: $R1 = 0.4\%$, $R2 = 19.4\%$, $R3 = 66.8\%$, $P1 = 13.4\%$, $P2 = 13.4\%$, $P3 = 13.4\%$)</p>

The second way is used by the ETRA nomogram [36] and the radar charts method [40]. In the ETRA nomogram [36], the calculated ratios of each of the gases to the gas with the highest concentration are plotted, and in the case of the radar charts method [40] the concentrations of the gases are plotted on each of the eight axes (the value used on the eighth axis is obtained from the equation in Table 9). Both methods produce a pattern, which should be compared with typical defect patterns to identify the type of failure.

The procedures for the square, heptagon, and two-shape graphical methods are given in Table 10. For methods using a square as a graphical representation, the relative percentages of four gases are plotted on the four sides of the square, creating a new square or a rectangle within the square. The intersection of the diagonals of the newly created square or rectangle is the point which, depending on the zone in which it is located, identifies the type of power transformer fault.

In the heptagon method [21], the relative percentages of the seven gases are calculated using the equations in Table 10. These equations give a weight to each of the gases, calculated by relating the typical concentrations of each gas to the CO concentration [21]. The relative percentages obtained are plotted on the seven sides of the heptagon, resulting in an irregular heptagon. The centroid of the irregular heptagon is calculated in a similar way to Mansour [41,48], but by placing the calculated relative percentages of each gas at the heads of the irregular heptagon. The area in which the centroid of this irregular heptagon is located identifies the type of fault in the transformer.

The first step in the two-shape graphical method [52] is to calculate the relative percentages of the five gases, this determines which of the two graphical shapes to use. If the percentage of C_2H_2 is less than or

equal to one, the square is used; if this percentage is greater than one, the pentagon is used. Once the shape has been selected, the percentages of the gases are placed on the heads of the square or pentagon and the centre of mass is calculated using the equations in Table 10. The fault type is identified by the zone in which the centre of mass is located.

The results of applying each of the methods to the two DGA results in Table 6 are shown in Table 11.

As the triangle developed by Bräsel and Sasum [23,24] uses C_3H_6 and C_3H_8 concentrations, and these concentrations were not available for any of the DGA samples in the database, it was not possible to apply the method.

Sample DGA 1 contains high concentrations of CH_4 and C_2H_6 , the latter being the highest concentration. According to Table 1, this gas pattern is characteristic of a thermal fault with temperature <300 °C. As shown in Table 6, sample DGA 1 was identified with a thermal fault in most cases. In some cases, this thermal fault was identified as T1, T2, O, or T1-O. The ETRA square identified sample DGA 1 as T3 or D+T. The result furthest from the majority is that obtained by the heptagon method, which identifies the defect as D2. However, the point identifying the fault is very close to the boundary between D2 and LCCD faults, which could suggest a possible modification of the heptagon.

Sample DGA 2 contains, in decreasing order, high concentrations of H_2 , C_2H_2 , and C_2H_4 . This gas pattern is indicative of low or high energy discharges, according to Table 1. All methods applied to sample DGA 2 identified the fault as an energy discharge. Those methods that discriminated between the energy level indicated whether it corresponded to D1 or D2. In these cases, most methods indicated a D2 fault.

Table 8
Procedures and equations for pentagon-shaped graphical methods.

Author	Year	Graph	Equation
Mansour [41]	2012		$x_m = \frac{1}{100} \sum_{i=1}^n m_i x_i$ $y_m = \frac{1}{100} \sum_{i=1}^n m_i y_i$ <p>x_i, y_i are the relative coordinates of each head of the pentagon, and m_i is the percentage concentration of each gas (Coordinate axis defined at the head of the pentagon relative to the acetylene. Side of the regular pentagon of 50 units. <u>No. 1:</u> $x_m = 39.24, y_m = -29.83$; <u>No. 2:</u> $x_m = 35.18, y_m = -2.27$)</p>
Duval and Lamarre [25,47] (DPM 1)	2014/2022	<p>First version</p> <p>Current version</p>	$C_x = \frac{1}{6A} \sum_{i=0}^{n-1} (x_i + x_{i+1})(x_i y_{i+1} - x_{i+1} y_i)$ $C_y = \frac{1}{6A} \sum_{i=0}^{n-1} (y_i + y_{i+1})(x_i y_{i+1} - x_{i+1} y_i)$ $A = \frac{1}{2} \sum_{i=0}^{n-1} (x_i y_{i+1} - x_{i+1} y_i)$ <p>x_i, y_i are the coordinates of the five points, A is the area of the irregular polygon, and C_x, C_y are the coordinates of the centroid (Coordinate axis defined at the centre of the pentagon. Distance of 40 units from the centre to each head of the pentagon. <u>No. 1:</u> $C_x = -20.96, C_y = -1.03$; <u>No. 2:</u> $C_x = 11.79, C_y = 6.63$)</p>
Mansour [48]	2015		<p>Procedure similar to Mansour [41] (Coordinate axis defined at the head of the pentagon relative to the acetylene. Side of the regular pentagon of 50 units. <u>No. 1:</u> $x_m = 39.24, y_m = -29.83$; <u>No. 2:</u> $x_m = 35.18, y_m = -2.27$)</p>

(continued on next page)

Table 8 (continued).

Author	Year	Graph	Equation
Duval [25,31] (DPM 2)	2016/ 2022	<p>First version</p> <p>Current version</p>	<p>Procedure similar to Duval and Lamarre [47] (DPM 1) (Coordinate axis defined at the centre of the pentagon. Distance of 40 units from the centre to each head of the pentagon. No. 1: $C_x = -20.96$, $C_y = -1.03$; No. 2: $C_x = 11.79$, $C_y = 6.63$)</p>
Cheim et al. [22]	2020		<p>Procedure similar to Duval and Lamarre [47] (DPM 1) (Coordinate axis defined at the centre of the pentagon. Distance of 40 units from the centre to each head of the pentagon. No. 1: $C_x = -20.96$, $C_y = -1.03$; No. 2: $C_x = 11.79$, $C_y = 6.63$)</p>

5. Discussion

Twenty-seven methods for identifying faults in power transformer oil were analysed in this review. All these methods have in common that they use a graphical representation to identify the type of fault. Traditional fault identification methods using gas ratios, such as RRM [7] or DRM [5,6] were not included in this review as these methods are already well known and covered in IEC [8] and IEEE [9] guides. The graphical fault identification methods found were reviewed because their implementation in any power transformer management system, as well as the subsequent interpretation of the results, is simple and intuitive.

In addition to several reviews of power transformer fault identification methods based on DGA results [63–65], this review includes all graphical methods found in the literature. Graphical methods collected from journal articles, conference proceedings, standards/guidelines, patents, and doctoral theses were reviewed. This review covers the period from 1970 to 2022. The first six methods analysed were developed in the period between 1970 and 1980, and the remaining twenty-one were developed from 1999 onwards.

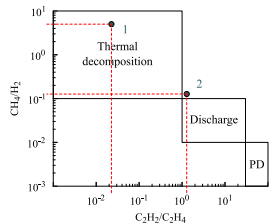
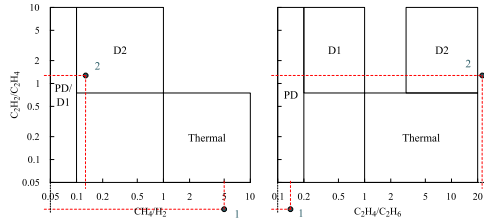
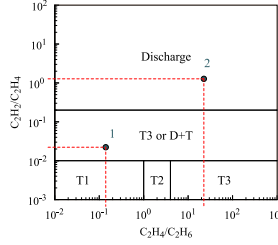
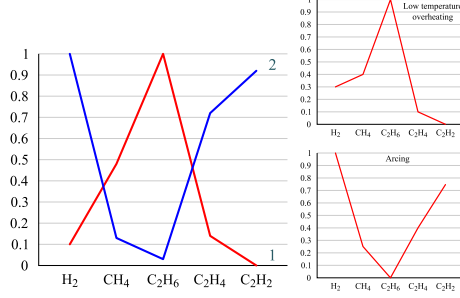
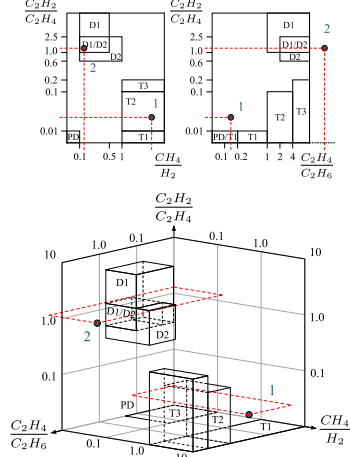
From this review it can be seen that the main gases used in most of the methods are the combustible gases obtained in the DGA, using from two (also using CO) to five combustible gases. CO and CO₂ gases, which indicate the degradation of solid insulation, are used in very few

methods. Finally, the use of C₃ hydrocarbon gases appears in only one of the methods reviewed.

All of the graphical methods examined identify discharges, thermal faults, and partial discharges. As the methods become more complex, they are able to separate the faults according to the energy level or temperature of the fault, and even show a mixture of both. However, it is interesting to note that only one method indicates a communicating OLTC or a leakage from an OLTC. As stated in [29], defining the communication between the main tank and the OLTC compartment is very important to avoid misdiagnosing faults in the power transformer. This may be an important point to consider in the development of new fault identification methods, either with graphical or gas ratio-based methods, or more complex methods using machine learning or deep learning. The current trend is to develop methods using machine learning and deep learning techniques. By applying these techniques, methods could be developed to identify communication between oil compartments in in-tank OLTC designs.

The application and implementation of each of the methods reviewed to diagnose the fault is one of the challenges developed in this work. The level of difficulty in creating algorithms from the methods is practically the same for all of them, with the most difficult part in some cases being the creation of the base figure used by the method. In terms of obtaining the diagnosis, the nomogram method and radar charts method are the most difficult to programme, as it is necessary

Table 9
Procedures and equations for graphical methods using 2-, 3-, or 8-axis charts or a nomogram.

Author	Year	Graph	Equation
Fallou et al. [10]	1970		$R1 = \frac{C_2H_2}{C_2H_4}$ $R2 = \frac{CH_4}{H_2}$ <p>H₂, CH₄, C₂H₂, and C₂H₄ are gas concentrations (ppm) (No. 1: R1 = 0.0222, R2 = 5 ; No. 2: R1 = 1.27, R2 = 0.127)</p>
Doernenburg and Hutzell [6]	1977		$R1 = \frac{C_2H_2}{C_2H_4}$ $R2 = \frac{CH_4}{H_2}$ $R3 = \frac{C_2H_4}{C_2H_6}$ <p>H₂, CH₄, C₂H₂, C₂H₄, and C₂H₆ are gas concentrations (ppm) (No. 1: R1 = 0.0222, R2 = 5, R3 = 0.14; No. 2: R1 = 1.27, R2 = 0.127, R3 = 22.6)</p>
ETRA [36,37] (ETRA square)	1980		$R1 = \frac{C_2H_2}{C_2H_4}$ $R2 = \frac{C_2H_4}{C_2H_6}$ <p>C₂H₂, C₂H₄, and C₂H₆ are gas concentrations (ppm) (No. 1: R1 = 0.0222, R2 = 0.14; No. 2: R1 = 1.27, R2 = 22.6)</p>
ETRA [36,38] (ETRA nomogram)	1980		<ol style="list-style-type: none"> Identify the gas with the highest concentration Calculate the ratio of each gas to the gas with the highest concentration Plot the gas ratios on the graph and connect the dots Compare the pattern with the reference patterns, and the best match identifies the fault <p>(No. 1: H₂ = 0.10, CH₄ = 0.48, C₂H₂ = 0, C₂H₄ = 0.14, C₂H₆ = 1; No. 2: H₂ = 1, CH₄ = 0.13, C₂H₂ = 0.92, C₂H₄ = 0.72, C₂H₆ = 0.03)</p>
IEC 60599 [8,33] (IRM)	1999		$R1 = \frac{C_2H_2}{C_2H_4}$ $R2 = \frac{CH_4}{H_2}$ $R5 = \frac{C_2H_4}{C_2H_6}$ <p>H₂, CH₄, C₂H₂, C₂H₄, and C₂H₆ are gas concentrations (ppm) (If no diagnosis can be given, the closest case is taken as the fault) (No. 1: R1 = 0.0222, R2 = 5, R5 = 0.14; No. 2: R1 = 1.27, R2 = 0.127, R5 = 22.6)</p>

(continued on next page)

Table 9 (continued).

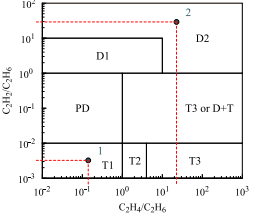
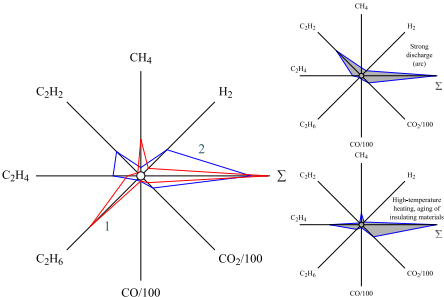
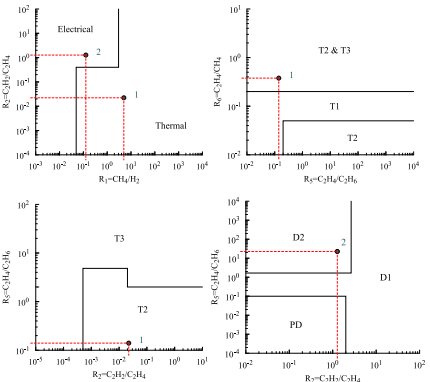
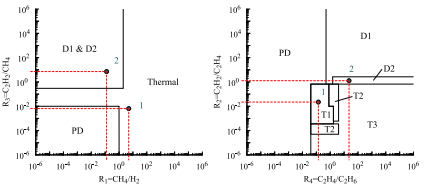
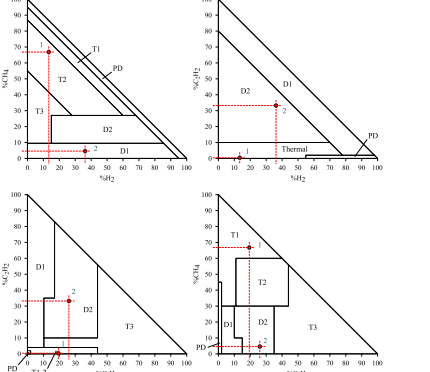
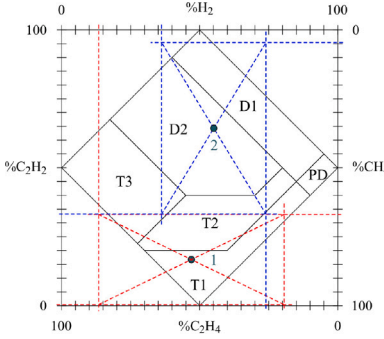
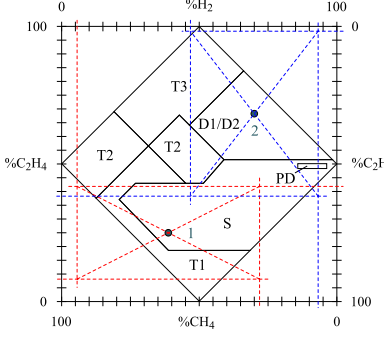
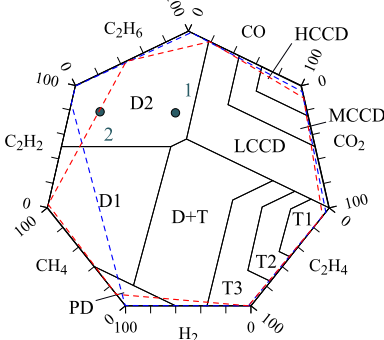
Author	Year	Graph	Equation
ETRA [37,39] (ETRA square 2)	1999		$R1 = \frac{C_2H_2}{C_2H_6}$ $R2 = \frac{C_2H_4}{C_2H_6}$ <p>C_2H_2, C_2H_4, and C_2H_6 are gas concentrations (ppm) (No. 1: $R1 = 0.00312$, $R2 = 0.14$; No. 2: $R1 = 28.8$, $R2 = 22.6$)</p>
Davydenko [40]	2013		<p>The equation used to calculate the sum of the gas concentrations (S) is:</p> $S = \sum_{m=1}^5 K_i + m(K_{CO} + K_{CO_2})$ <p>K_i are the concentrations of combustible gases (ppm), m is a scaling factor ($m = 0.01$), and K_{CO} and K_{CO_2} are the concentrations of CO and CO₂ (ppm) respectively. The best match when comparing the obtained pattern with the reference patterns indicates the fault. (No. 1 : $S = 586.73$ ppm; No. 2 : $S = 506.43$ ppm)</p>
Kim et al. [43]	2013		$R1 = \frac{CH_4}{H_2}$ $R2 = \frac{C_2H_2}{C_2H_4}$ $R5 = \frac{C_2H_2}{C_2H_6}$ $R6 = \frac{C_2H_4}{CH_4}$ <p>H_2, CH_4, C_2H_2, C_2H_4, and C_2H_6 are gas concentrations (ppm) (No. 1: $R1 = 5$, $R2 = 0.0222$, $R5 = 0.14$, $R6 = 0.29$; No. 2: $R1 = 0.127$, $R2 = 1.27$, $R5 = 22.6$)</p>
Kim et al. [44,45]	2013		$R1 = \frac{CH_4}{H_2}$ $R2 = \frac{C_2H_2}{C_2H_4}$ $R3 = \frac{C_2H_2}{CH_4}$ $R4 = \frac{C_2H_4}{C_2H_6}$ <p>H_2, CH_4, C_2H_2, C_2H_4, and C_2H_6 are gas concentrations (ppm) (No. 1: $R1 = 5$, $R2 = 0.0222$, $R3 = 0.00645$, $R4 = 0.14$; No. 2: $R1 = 0.127$, $R2 = 1.27$, $R3 = 7.2$, $R4 = 22.6$)</p>
Lee et al. [46]	2013		$\%C_2H_2 = \frac{100w}{w+x+y+z}$ $\%C_2H_4 = \frac{100x}{w+x+y+z}$ $\%CH_4 = \frac{100y}{w+x+y+z}$ $\%H_2 = \frac{100z}{w+x+y+z}$ <p>w, x, y, and z are the concentrations of C_2H_2, C_2H_4, CH_4, and H_2 (ppm) respectively (If the results of each combination are different, a fault diagnosis is made based on the weight values of the diagnosed faults given in [46]) (No. 1: $\%C_2H_2 = 0.4\%$, $\%C_2H_4 = 19.4\%$, $\%CH_4 = 66.8\%$, $\%H_2 = 13.4\%$; No. 2: $\%C_2H_2 = 33.2\%$, $\%C_2H_4 = 26\%$, $\%CH_4 = 4.6\%$, $\%H_2 = 36.2\%$)</p>

Table 10
Procedures and equations for square, heptagon, and two-shape graphical methods.

Author	Year	Graph	Equation
Lee et al. [46]	2013		$\%C_2H_2 = \frac{100 \cdot w}{w+x+y+z}$ $\%C_2H_4 = \frac{100 \cdot x}{w+x+y+z}$ $\%CH_4 = \frac{100 \cdot y}{w+x+y+z}$ $\%H_2 = \frac{100 \cdot z}{w+x+y+z}$ <p>$w, x, y,$ and z are the concentrations of $C_2H_2, C_2H_4, CH_4,$ and H_2 (ppm) respectively No. 1: $\%C_2H_2 = 0.4\%, \%C_2H_4 = 19.4\%, \%CH_4 = 66.8\%, \%H_2 = 13.4\%$ No. 2: $\%C_2H_2 = 33.2\%, \%C_2H_4 = 26\%, \%CH_4 = 4.6\%, \%H_2 = 36.2\%$</p>
Kim and Seo [49,50]	2017		$\%C_2H_6 = \frac{100 \cdot w}{w+x+y+z}$ $\%C_2H_4 = \frac{100 \cdot x}{w+x+y+z}$ $\%CH_4 = \frac{100 \cdot y}{w+x+y+z}$ $\%H_2 = \frac{100 \cdot z}{w+x+y+z}$ <p>$w, x, y,$ and z are the concentrations of $C_2H_6, C_2H_4, CH_4,$ and H_2 (ppm) respectively No. 1: $\%C_2H_6 = 58.15\%, \%C_2H_4 = 8.15\%, \%CH_4 = 28.08\%, \%H_2 = 5.62\%$ No. 2: $\%C_2H_6 = 1.7\%, \%C_2H_4 = 38.3\%, \%CH_4 = 6.8\%, \%H_2 = 53.2\%$</p>
Gouda et al. [21]	2018		$\%H_2 = \frac{3.5 \cdot H_2 \cdot 100}{3.5 \cdot H_2 + 2.9167 \cdot CH_4 + 5.3846 \cdot C_2H_6 + 7 \cdot C_2H_4 + 116.6667 \cdot C_2H_2 + CO + 0.14 \cdot CO_2}$ $\%CH_4 = \frac{2.9167 \cdot CH_4 \cdot 100}{3.5 \cdot H_2 + 2.9167 \cdot CH_4 + 5.3846 \cdot C_2H_6 + 7 \cdot C_2H_4 + 116.6667 \cdot C_2H_2 + CO + 0.14 \cdot CO_2}$ $\%C_2H_6 = \frac{5.3846 \cdot C_2H_6 \cdot 100}{3.5 \cdot H_2 + 2.9167 \cdot CH_4 + 5.3846 \cdot C_2H_6 + 7 \cdot C_2H_4 + 116.6667 \cdot C_2H_2 + CO + 0.14 \cdot CO_2}$ $\%C_2H_4 = \frac{7 \cdot C_2H_4 \cdot 100}{3.5 \cdot H_2 + 2.9167 \cdot CH_4 + 5.3846 \cdot C_2H_6 + 7 \cdot C_2H_4 + 116.6667 \cdot C_2H_2 + CO + 0.14 \cdot CO_2}$ $\%C_2H_2 = \frac{116.6667 \cdot C_2H_2 \cdot 100}{3.5 \cdot H_2 + 2.9167 \cdot CH_4 + 5.3846 \cdot C_2H_6 + 7 \cdot C_2H_4 + 116.6667 \cdot C_2H_2 + CO + 0.14 \cdot CO_2}$ $\%CO = \frac{CO \cdot 100}{3.5 \cdot H_2 + 2.9167 \cdot CH_4 + 5.3846 \cdot C_2H_6 + 7 \cdot C_2H_4 + 116.6667 \cdot C_2H_2 + CO + 0.14 \cdot CO_2}$ $\%CO_2 = \frac{0.14 \cdot CO_2 \cdot 100}{3.5 \cdot H_2 + 2.9167 \cdot CH_4 + 5.3846 \cdot C_2H_6 + 7 \cdot C_2H_4 + 116.6667 \cdot C_2H_2 + CO + 0.14 \cdot CO_2}$ <p>$H_2, CH_4, C_2H_2, C_2H_4, C_2H_6, CO,$ and CO_2 are gas concentrations (ppm) Plot the relative percentage of each gas on the heptagon graph, then the corresponding point identifying the fault corresponds to the centre of mass of the relative percentage concentrations (No. 1 (red dashed line): $\%H_2 = 2.8\%, \%CH_4 = 11.8\%, \%C_2H_6 = 45.3\%, \%C_2H_4 = 8.2\%, \%C_2H_2 = 3.1\%, \%CO = 19.1\%, \%CO_2 = 9.7\%$; No. 2 (blue dashed line): $\%H_2 = 2.8\%, \%CH_4 = 0.3\%, \%C_2H_6 = 0.1\%, \%C_2H_4 = 4.0\%, \%C_2H_2 = 85.8\%, \%CO = 2.5\%, \%CO_2 = 4.5\%$)</p>

(continued on next page)

Table 10 (continued).

Author	Year	Graph	Equation
Emara et al. [52]	2021		$S = \sum_{i=1}^5 (P_i)$ $P_{\%i} = \frac{P_i}{S} * 100$ <p>P_i is the concentration of each gas (ppm), S is the sum of the concentrations of the five gases (ppm), and $P_{\%i}$ is the relative percentage of each gas.</p> <p>If $P_{\%C_2H_2} \leq 1\%$, the square is used and if $P_{\%C_2H_2} > 1\%$, the pentagon is used.</p> <p>The centre of mass (x_m, y_m) for the four or five heads, indicating the type of fault, is calculated using the following equations:</p> $x_m = \frac{1}{\sum_{i=1}^n P_{\%i}} \sum_{i=1}^n (P_{\%i} x_i)$ $y_m = \frac{1}{\sum_{i=1}^n P_{\%i}} \sum_{i=1}^n (P_{\%i} y_i)$ <p>x_i and y_i are the polygon head coordinates, and n is the number of gases (four or five depending on the shape).</p> <p>(Coordinate axis defined at the head relative to hydrogen in the square and at the head relative to acetylene in the pentagon. Side of the square and the regular pentagon of 50 units. <u>No. 1</u> (square): $x_m = 33.15, y_m = 18.12$; <u>No. 2</u> (pentagon): $x_m = 35.18, y_m = -2.27$)</p>

to compare the pattern obtained with the reference patterns. In this review, this task was performed manually as only two DGA results were used. However, it would be necessary to develop a system similar to that proposed by Shutenko and Jakovenko [57] in order to incorporate it into a power transformer management system.

One of the features that motivated this review was that these graphical methods generally allow the evolution of the faults of the same transformer to be obtained visually by plotting successive DGA results on the same method. In this respect, the nomograph, the nomogram, and the radar charts method do not allow the evolution of the fault to be obtained, whereas the other twenty-four methods analysed do.

Regarding the application of the analysed graphical methods to two real DGA results of power transformers in service, it should be noted that this work does not aim to define which of them has the best accuracy, since only two DGA results were used. As shown in Table 11, the two DGA results analysed using the twenty-seven methods allowed the fault to be identified, with the exception of the method developed by Bräsel and Sasum [23,24]. As mentioned, this method uses C₃ hydrocarbon gases, which are not available in the database to which the authors have access.

All of the methods presented in this review result in the identification of one type of fault or a mixture of faults, whereas in reality several types of faults can occur simultaneously. This is because the graphical diagnostic methods reviewed use deterministic boundaries to separate the different fault types and severities. They do not take into account or allow interpretation of gas concentrations as the sum of gases generated in two different faults occurring simultaneously, for example. One of the possible lines of research in power transformer fault identification methods using DGA would be the development of new AI-based methods that would be able to detect the presence of multiple types of faults in the power transformer simultaneously. The main problem or limitation in the development of this type of AI-based method is the training of the model, which requires a large amount of data. To date, there is no database or results presented in articles with the necessary volume to train the model that faithfully captures the relationship between DGA results and the reliable presence of multiple faults in the transformer.

6. Conclusions

This review has analysed the literature on fault identification methods for oil-immersed power transformers, focusing on those methods that have a graphical representation because their implementation in any power transformer management system, as well as their subsequent interpretation of the results, is simple and intuitive. Twenty-seven graphical fault identification methods developed between 1970 and 2023 were found.

The review identified a number of key features of the graphical methods, such as the number of gases used, the form of the graphical representation, the number of faults identifiable, and the types of data used from the gas concentrations obtained in the DGA.

This review shows the procedures and equations for the application of the twenty-seven methods analysed to identify the type of fault in the power transformer. To better illustrate the procedures of each method, two real DGA samples of two in-service power transformers were used in the application of the methods. As indicated, the application of each method using two DGA results and the identification of the fault is not intended to indicate the accuracy of the methods or to obtain a ranking of the best methods, since only two DGA samples were used. What can be deduced from the application of the twenty-seven methods is that almost all of them detected that the first sample indicated a thermal fault and the second a discharge fault.

This work is intended to be a starting point for the development of new fault identification methods that can combine graphical methods with AI techniques. As it is a comprehensive review of graphical methods for fault identification in oil-immersed power transformers, this review can help in the selection or comparison of methods to be used in the development of new AI-based methods.

From the review of the graphical fault identification methods, it can be seen that the most widely used method is DTM 1. Although it is one of the oldest methods, it is the most widely used, either for simple fault identification or as a basis for the development of new AI-based models. It is also the main method used in most of the newly developed methods to compare their accuracy, which shows that it is still the main method to overcome. Another method used to develop new methods based on it, or to compare the accuracy results of new methods, is DPM 1.

Table 11
Results of the faults identified by the graphical methods.

Author	Faults identified	
	Sample 1	Sample 2
Fallou et al. [10] ^a	Thermal	Discharge ^j
Duval [11,26,32,33] (DTM 1) ^b	T2	D2-H
Church et al. [34,35] (Nomograph) ^c	Thermal ^k	Arcing
Doernenburg and Hutzl [6] ^a	Thermal ^j	D2 ^j
ETRA [36,37] (ETRA Square) ^a	T3 or D+T	Discharge
ETRA [36,38] (Nomogram) ^d	T1 ^l	D2 ^l
IEC 60599 [8,33] (IRM) ^{a,e}	T1 ^j	D1/D2 ^j
ETRA [37,39] (ETRA Square 2) ^a	T1	D2
Duval [27,28] (DTM 4) ^b	O	m
Duval [27,28] (DTM 5) ^b	O	n
Bräsel and Sasum [23,24] ^b	o	o
Davydenko [40] ^f	Thermal ^p	Arcing ^p
Mansour [41] ^g	T1	D2
Moodley and Gaunt [42] ^b	T1	D2
Kim et al. [43] ^a	T2	D2
Kim et al. [44,45] ^a	T1	D2
Lee et al. [46] ^h	T1	D2
Lee et al. [46] ^a	T1	D2
Duval and Lamarre [25,47] (DPM 1) ^g	T1	D2-H
Mansour [48] ^g	T1	D2
Duval [25,31] (DPM 2) ^g	O	D2-H
Spremic [30] ^b	T1	D2
Kim and Seo [49,50] ^h	S	D1/D2
Gouda et al. [21] ⁱ	D2	D2
Gouda et al. [51] ^b	T2	D2
Cheim et al. [22] ^g	T1-O	D2
Emara et al. [52] ^{g,h}	T1	D2

^a Shapes: 2-axis

^b Shapes: triangle

^c Shapes: nomograph

^d Shapes: nomogram

^e Shapes: 3-axis

^f Shapes: 8-axis

^g Shapes: pentagon

^h Shapes: square

ⁱ Shapes: heptagon

^j Identified fault closest to the case

^k The method also indicates the accelerated decomposition rate of the solid insulation

^l Identification of faults by comparison with reference patterns of defect types

^m Method not used for the type of faults identified as D1, D2, or T3 in DTM 1

ⁿ Method not used for the type of faults identified as D1 or D2 in DTM 1

^o It was not possible to obtain a diagnosis because not all required gas concentrations (C₂H₆ and C₃H₈) were available

^p Identification of faults by comparison with radar chart patterns of defect types.

CRedit authorship contribution statement

Sergio Bustamante: Conceptualization, Methodology, Software, Validation, Formal analysis, Investigation, Resources, Writing – original draft. **Mario Manana:** Conceptualization, Validation, Formal analysis, Resources, Writing – review & editing, Funding acquisition. **Alberto Arroyo:** Conceptualization, Validation, Formal analysis, Resources, Writing – review & editing. **Alberto Laso:** Validation, Formal analysis, Writing – review & editing. **Raquel Martinez:** Validation, Formal analysis, Writing – review & editing.

Declaration of competing interest

The authors declare that they have no known competing financial interests or personal relationships that could have appeared to influence the work reported in this paper.

Data availability

No data was used for the research described in the article.

Acknowledgement

The authors acknowledge the support received from EDP Redes España.

Funding

This study was partially funded by the FLEXIGRID project from the European Union's Horizon 2020 research and innovation programme [grant number 864579].

References

- [1] Wani SA, Rana AS, Sohail S, Rahman O, Parveen S, Khan SA. Advances in DGA based condition monitoring of transformers: A review. *Renew Sustain Energy Rev* 2021;149:111347.
- [2] AJ C, Salam M, Rahman Q, Wen F, Ang S, Voon W. Causes of transformer failures and diagnostic methods – A review. *Renew Sustain Energy Rev* 2018;82:1442–56.
- [3] Azmi A, Jasni J, Azis N, Kadir MA. Evolution of transformer health index in the form of mathematical equation. *Renew Sustain Energy Rev* 2017;76:687–700.
- [4] de Faria H, Costa JGS, Olivas JLM. A review of monitoring methods for predictive maintenance of electric power transformers based on dissolved gas analysis. *Renew Sustain Energy Rev* 2015;46:201–9.
- [5] Dornenburg E, Strittmatter W. Monitoring oil cooled transformers by gas analysis. *Brown Boveri Rev* 1974;61(5):238–47.
- [6] Dornenburg E, Hutzl O. Operational supervision by testing the insulating oil. *Elektrotechnische Z / A* 1977;98(3):211–5.
- [7] Rogers RR. IEEE and IEC codes to interpret incipient faults in transformers, using gas in oil analysis. *IEEE Trans Electr Insul* 1978;EI-13(5):349–54.
- [8] IEC. Mineral oil-filled electrical equipment in service – Guidance on the interpretation of dissolved and free gases analysis. 2022, IEC 60599:2022.

- [9] IEEE. IEEE guide for the interpretation of gases generated in mineral oil-immersed transformers. In: IEEE Std C57.104-2019 (Revision of IEEE Std C57.104-2008). 2019, p. 1–98.
- [10] Fallou B, Davies I, Rogers R, Reynolds E, Viale F, Devaux A, et al. Application of physico-chemical methods of analysis to the study of deterioration in the insulation of electrical apparatus. In: CIGRE. 1970, Paper 15-07.
- [11] Duval M. Fault gases formed in oil-filled breathing EHV power transformers. The interpretation of gas analysis data. In: IEEE-PES conf. 1974, Paper C 74-476-8.
- [12] CIGRE. Advances in DGA interpretation. In: JWG D1/A2.47, Technical Brochure no. 771. 2019.
- [13] Badawi M, Ibrahim SA, Mansour D-EA, El-Faraskoury AA, Ward SA, Mahmoud K, et al. Reliable estimation for health index of transformer oil based on novel combined predictive maintenance techniques. *IEEE Access* 2022;10:25954–72.
- [14] Wani SA, Gupta D, Farooq MU, Khan SA. Multiple incipient fault classification approach for enhancing the accuracy of dissolved gas analysis (DGA). *IET Sci Meas Technol* 2019;13(7):959–67.
- [15] Badawi M, Ibrahim SA, EL-Faraskoury A, Mansour D-EA, Ward SA. A novel DGA oil interpretation approach based on combined techniques. In: 2022 23rd international middle east power systems conference. 2022, p. 01–8. <http://dx.doi.org/10.1109/MEPCON55441.2022.10021795>.
- [16] Gouda OE, El-Hoshy SH, Ghoneim SSM. Enhancing the diagnostic accuracy of DGA techniques based on IEC-TC10 and related databases. *IEEE Access* 2021;9:118031–41.
- [17] Rokani V, Kaminaris SD, Karaisas P, Kaminaris D. Power transformer fault diagnosis using neural network optimization techniques. *Mathematics* 2023;11(22).
- [18] Yang D, Qin J, Pang Y, Huang T. A novel double-stacked autoencoder for power transformers DGA signals with an imbalanced data structure. *IEEE Trans Ind Electron* 2022;69(2):1977–87.
- [19] Taha IBM, Ibrahim S, Mansour D-EA. Power transformer fault diagnosis based on DGA using a convolutional neural network with noise in measurements. *IEEE Access* 2021;9:111162–70.
- [20] Msomi NL, Thango BA. Development of dissolved gas analysis-based fault identification system using machine learning with google colab. In: 2023 31st southern african universities power engineering conference. 2023, p. 1–6. <http://dx.doi.org/10.1109/SAUPEC57889.2023.10057713>.
- [21] Gouda OE, El-Hoshy SH, El-Tamaly HH. Proposed heptagon graph for DGA interpretation of oil transformers. *IET Gener Transm Distrib* 2018;12(2):490–8.
- [22] Cheim L, Duval M, Haider S. Combined duval pentagons: A simplified approach. *Energies* 2020;13(11):2859.
- [23] Bräsel E, Sasum U. Online Transformer Gas Diagnostics on the Basis of IEC 60567/60599. In: International conference on power transformers. 2009, p. 89–93.
- [24] Bräsel E, Sasum U. Universal Fault Triangle in Transformer Diagnostics. 2009, p. 70–5, ew.
- [25] Duval M, Buchacz J. Identification of arcing faults in paper and oil in transformers—Part I: Using the Duval pentagons. *IEEE Electr Insul Mag* 2022;38(1):19–23.
- [26] Duval M, Buchacz J. Gas formation from arcing faults in transformers—Part II. *IEEE Electr Insul Mag* 2022;38(6):12–5.
- [27] Duval M. The duval triangle for load tap changers, non-mineral oils and low temperature faults in transformers. *IEEE Electr Insul Mag* 2008;24(6):22–9.
- [28] Duval M. New frontiers of DGA interpretation for power transformers and their accessories. In: Society of electrical and electronics engineers. 2013, p. 1–8.
- [29] Bustamante S, Manana M, Arroyo A, Laso A, Martinez R. Determination of transformer oil contamination from the OLTC gases in the power transformers of a distribution system operator. *Appl Sci* 2020;10(24):8897.
- [30] Spremic S. Improvement of duval triangle 1. In: Congrès international des Réseaux électriques de distribution. 2017.
- [31] Duval M. Use of Duval Pentagons and Triangles for the Interpretation of DGA in Electrical Equipment. In: Proceedings of the TechCon North America conference. 2016, p. 58–82.
- [32] Duval M. Dissolved gas analysis: It can save your transformer. *IEEE Electr Insul Mag* 1989;5(6):22–7.
- [33] IEC. Mineral oil-impregnated electrical equipment in service – Guide to the interpretation of dissolved and free gases analysis. 1999, IEC 60599:1999.
- [34] Church JO, Hauptert TO, Jakob F. Analyze Incipient Faults with Dissolved Gas Nomenclature. *Electr World* 1987;201(10):40–4.
- [35] Hauptert TJ, Jakob F. A Review of the Operating Principles and Practice of Dissolved Gas Analysis. *Electr Insulations Oils* 1988;STP 998:108–15.
- [36] Electric Technology Research Association. Maintenance management of oil-filled equipment by gas-in-oil analysis. *Electr Technol Res* 1980;36(1).
- [37] Mori E, Taukioka H, Takamoto K, Miyamoto N, Kobayashi T, Kobayashi S, et al. Latest diagnostic methods of gas-in-oil analysis for oil-filled transformer in Japan. In: Proceedings of 1999 IEEE 13th international conference on dielectric liquids (ICDL'99) (cat. no.99CH36213). 1999, p. 503–8. <http://dx.doi.org/10.1109/ICDL.1999.798982>.
- [38] Kawamura T, Yamaoka M, Kawada H, Ando K, Maeda T, Takatsu T. Analyzing gases dissolved in oil and its application to maintenance of transformers. In: CIGRE international conference on large high voltage electric systems. 1986, Paper 12–05.
- [39] Electric Technology Research Association. Maintenance management of oil-filled equipment by gas-in-oil analysis. *Electr Technol Res* 1999;54(5).
- [40] Davidenko I. Development of a system for multiple assessment of technical condition and maintenance of high-voltage oil-filled electrical equipment [Ph.D. thesis], Yekaterinburg: Ural State Technical University; 2009.
- [41] Mansour D-EA. A new graphical technique for the interpretation of dissolved gas analysis in power transformers. In: 2012 annual report conference on electrical insulation and dielectric phenomena. 2012, p. 195–8. <http://dx.doi.org/10.1109/CEIDP.2012.6378754>.
- [42] Moodley N, Gaunt C. Developing a power transformer low energy degradation assessment triangle. In: IEEE power and energy society conference and exposition in Africa: intelligent grid integration of renewable energy resources. 2012, p. 1–6. <http://dx.doi.org/10.1109/PowerAfrica.2012.6498647>.
- [43] Kim S-W, Kim S-J, Seo H-D, Jung J-R, Yang H-J, Duval M. New methods of DGA diagnosis using IEC TC 10 and related databases Part 1: application of gas-ratio combinations. *IEEE Trans Dielectr Electr Insul* 2013;20(2):685–90.
- [44] Kim S-W, Seo H-D, Kim S-J. Method for diagnosing internal fault of oil-immersed transformer through composition ratio of dissolved gas in oil, (no. WO2013100591A1). Hyosung Corporation; 2013, World Intellectual Property Organization (Patent Cooperation Treaty) Patent, URL: <https://patents.google.com/patent/WO2013100591A1/en>.
- [45] Kim S-W, Seo H-D, Kim S-J. Method for diagnosing internal fault of oil-immersed transformer through composition ratio of dissolved gas in oil, (no. US9599653B2). Hyosung Corporation; 2017, US Patent, URL: <https://patents.google.com/patent/US9599653B2/en>.
- [46] Lee S-J, Kim Y-M, Seo H-D, Jung J-R, Yang H-J, Duval M. New methods of DGA diagnosis using IEC TC 10 and related databases Part 2: application of relative content of fault gases. *IEEE Trans Dielectr Electr Insul* 2013;20(2):691–6.
- [47] Duval M, Lamarre L. The duval pentagon-a new complementary tool for the interpretation of dissolved gas analysis in transformers. *IEEE Electr Insul Mag* 2014;30(6):9–12.
- [48] Mansour D-EA. Development of a new graphical technique for dissolved gas analysis in power transformers based on the five combustible gases. *IEEE Trans Dielectr Electr Insul* 2015;22(5):2507–12.
- [49] Kim S-J, Seo H-D. Method for diagnosing oil-immersed transformer, (no. WO2017116091A1). Hyosung Corporation; 2017, World Intellectual Property Organization (Patent Cooperation Treaty) Patent, URL: <https://patents.google.com/patent/WO2017116091A1/en>.
- [50] Kim S-J, Seo H-D. Method for diagnosing oil-immersed transformer, (no. KR101772914B1). Hyosung Corporation; 2017, Korean Patent, URL: <https://patents.google.com/patent/KR101772914B1/en>.
- [51] Gouda OE, El-Hoshy SH, E.L.-Tamaly HH. Condition assessment of power transformers based on dissolved gas analysis. *IET Gener Transm Distrib* 2019;13(12):2299–310.
- [52] Emara MM, Peppas GD, Gonos IF. Two graphical shapes based on DGA for power transformer fault types discrimination. *IEEE Trans Dielectr Electr Insul* 2021;28(3):981–7.
- [53] Moodley N, Gaunt CT. Low energy degradation triangle for power transformer health assessment. *IEEE Trans Dielectr Electr Insul* 2017;24(1):639–46.
- [54] Guidelines for the diagnosis of developing faults in transformer equipment based on the results of the chromatographic analysis of gases dissolved in oil. 2001, RD 153-34.0-46.302-00.
- [55] Guidelines for the technical diagnosis of developing defects in oil-filled high-voltage electrical equipment based on the analysis of gases dissolved in mineral transformer oil. 2001, Organization standard STO 4.01-23-003-2019.
- [56] Diagnosis oil-filled transformer equipment based on the results of chromatographic analysis of free gas with gas relay selected, and gases dissolved in insulating oil. 2007, SOU-N EE 46.501.
- [57] Oleg S, Ivan J. Fault diagnosis of power transformer using method of graphic images. In: 2017 IEEE international Young scientists forum on applied physics and engineering. 2017, p. 66–9. <http://dx.doi.org/10.1109/YSF.2017.8126594>.
- [58] Bhalla D, Bansal RK, Gupta HO. Application of artificial intelligence techniques for dissolved gas analysis of transformers-A review. *Int J Electr Comput Eng* 2010;4(2):261–9.
- [59] Kim S-J, Seo H-D, Kim Y-M. Fault diagnosis method of oil filled transformer using proportion ratio of dissolved gases, (no. KR101290806B1). Hyosung Corporation; 2013, Korean Patent, URL: <https://patents.google.com/patent/KR101290806B1/en>.
- [60] Kim Y-M, Kim S-J, Seo H-D, Lee S-J. Method for diagnosing internal fault of oil-immersed transformer through content ratios of dissolved gases, (no. WO2013100593A1). Hyosung Corporation; 2013, World Intellectual Property Organization (Patent Cooperation Treaty) Patent, URL: <https://patents.google.com/patent/WO2013100593A1/en>.
- [61] Kim Y-M, Kim S-J, Seo H-D, Lee S-J. Method for diagnosing internal fault of oil-immersed transformer through content ratios of dissolved gases, (no. US9535134B2). Hyosung Corporation; 2017, US Patent, URL: <https://patents.google.com/patent/US9535134B2/en>.
- [62] Kim Y-M, Seo H-D, Lee S-J. Fault Diagnosis Method of Oil Filled Transformer using Proportion Ratio Combination of Dissolved Gases, (no. KR101290295B1). Hyosung Corporation; 2013, Korean Patent, URL: <https://patents.google.com/patent/KR101290295B1/en>.

- [63] Faiz J, Soleimani M. Dissolved gas analysis evaluation in electric power transformers using conventional methods a review. *IEEE Trans Dielectr Electr Insul* 2017;24(2):1239–48.
- [64] Kulyk O. Analysis of the diagnostic criteria used to defect type recognition based on the results of analysis of gases dissolved in oil. *Bull Natl Tech Univ "KhPI". Ser Energy Reliab Energy Effic* 2020;1(1):15–25.
- [65] Shutenko O, Kulyk O, Ponomarenko S. Comparative analysis of existing standards and methodologies for interpreting DGA results: study guide for individual computational and graphical tasks. *Kharkiv: National technical university "Kharkiv polytechnic institute";* 2021.

Sergio Bustamante received the B.Sc. in Energy Resources Engineering and the M.Sc. in Mining Engineering Specialized in Energy from the Universidad de Cantabria, Spain, in 2014 and 2017, respectively. He received his Ph.D. in Industrial Engineering from Universidad de Cantabria, Spain, in 2022. Since 2016, he has been a Research Assistant with the Department of Electrical and Energy Engineering in Advanced Electro-Energetic Technology Group (GTEA). His research interests include electrical asset maintenance and dynamic management of high- and medium-voltage underground cables.

Mario Manana received the B.S. degree in Telecommunications Engineering from the University of Alcalá, Spain, in 1992 and the M.S. (with Distinction) and Ph.D. degrees in Telecommunications Engineering from the Universidad de Cantabria, Santander, Spain, in 1995 and 2000, respectively. From 2005 to 2012, he has been the head of the Department of Electrical and Energy Engineering, Universidad de Cantabria. From 2012 to 2016, he has been director of the Sustainability Office attached to the Vice-Chancellor of Campus, Services and Sustainability. Since March 2016, he is the Vice-Chancellor of Campus, Services and Sustainability (UC). He also works as a Lecturer and Researcher with the Department of Electrical and Energy Engineering; he leads the Advanced Electro-Energetic Technology Group (GTEA) and, from 2016

to 2019, the Viesgo Energy Chair. He is Full Professor of electrical engineering. His research interests include power quality, energy efficiency, and grid-integration of renewable energies.

Alberto Arroyo received the B.Sc.+M.Sc. in Industrial Engineering and the Ph.D. in Electrical Engineering from the Universidad de Cantabria, Santander, Spain, in 2007 and 2012, respectively. Currently, he is an Associate Professor in the Department of Electrical and Energy Engineering at the Universidad de Cantabria. He has the head of the Department of Electrical and Energy Engineering, Universidad de Cantabria since 2020. He has published 3 chapters in international books, 27 works in international conferences, and 15 papers in journals included in the Journal of Citation Report. He has worked as an Electrical Engineer at Gamesa Electric.

Alberto Laso received his Telecommunications Engineer Degree at the Universidad de Cantabria, Spain, in 2008. He also received a M.Sc. in Research in Industrial Engineering in 2015 by the same university. After that, he reached his Ph.D. in Industrial Engineering from Universidad de Cantabria, Spain, in 2021. He has been working as a Research Assistant in the Department of Electrical and Energy Engineering in Advanced Electro-Energetic Technology Group (GTEA) since 2013. In 2023, he continues in the same department and research group as Assistant Professor. Additionally, he worked as a Telecommunication Engineer in CRV Consulting and Services from 2009 to 2011.

Raquel Martinez received her BSc+MSc in Industrial Engineering and her M.Sc. in Research in Industrial Engineering from Universidad de Cantabria, Spain, in 2011 and 2012, respectively. She received her Ph.D. in Industrial Engineering from Universidad de Cantabria, Spain, in 2016. After that, she has continued her work as Researcher in the Department of Electrical and Energy Engineering in Advanced Electro-Energetic Technology Group (GTEA). In 2023, she is still in the same department and research group as Assistant Professor.